

ROOF SYSTEMS BEHAVIOR

Progress Report

PREDICTION OF LATERAL RESTRAINT FORCES
FOR Z-PURLIN SUPPORTED ROOF SYSTEMS

by

Souhail Elhouar
and
Thomas M. Murray
Principal Investigator

Sponsored by

Metal Building Manufacturers Association
and
American Iron and Steel Institute

Report No. FSEL/MBMA 85-03

May 1985

FEARS STRUCTURAL ENGINEERING LABORATORY
School of Civil Engineering and Environmental Science
University of Oklahoma
Norman, Oklahoma 73019

ABSTRACT

The objective of this study was to develop a design procedure for lateral restraint requirements for thru fastener, corrugated steel panel, multiple purlin line, multiple span roof systems. For this purpose, a stiffness model was developed and calibrated to fit a set of prototype and quarter scale experimental test results. The model was then used to predict lateral restraint forces for a wide range of systems with either torsional restraint, third point span restraint, or midspan restraint. Further, a parametric study was conducted and regression analyses performed on the collected data. The resulting prediction equations are the basis for a proposed design procedure. Design examples are given at the end of the thesis.

ACKNOWLEDGEMENTS

The research reported here was sponsored by the Metal Building Manufacturers Association and by the American Iron and Steel Institute under the guidance of the MBMA Roof Systems Behavior Research Subcommittee.

The contents of this report are essentially the same as the thesis submitted by Souhail Elhouar to the faculty of the School of Civil Engineering and Environmental Science, University of Oklahoma, in partial fulfillment of the requirements for the degree of Master of Science.

TABLE OF CONTENTS

ABSTRACT	Page iii
ACKNOWLEDGEMENTS	iv
LIST OF FIGURES	vii
LIST OF TABLES	x
CHAPTER	
I. INTRODUCTION AND LITERATURE REVIEW	1
1.1 Scope	1
1.2 Review of Previous Research	3
1.3 Current Design Practice	10
1.4 Conclusions and Justification of Study	10
II. DEVELOPMENT OF A MATHEMATICAL MODEL	12
2.1 Overview	12
2.2 Mathematical Modeling	14
2.2.1 Modeling of the Purlin	16
2.2.2 Modeling of the Panel	16
2.2.3 Modeling of the Braces	19
2.2.4 Cross-Sectional Properties of the Purlin Members	20
2.2.5 Applied Load	20
2.3 Method of Solution	23
2.4 Comparison with Other Analytical Models	23
III. COMPARISON OF ANALYTICAL RESULTS WITH TEST RESULTS	25
3.1 Testing Configurations and Test Series	25
3.2 Conclusions	33
IV. DEVELOPMENT OF THE DESIGN PROCEDURE	34
4.1 Methodology	34
4.2 Limits of Parameters and Configurations	34
4.3 Development of the Design Equations	35
4.3.1 Cross Sections Used	35
4.3.2 System Behavior Analysis	39
4.3.3 Regression Analysis	53
4.4 Conclusions	64

V. DESIGN PROCEDURE AND EXAMPLES	65
5.1 General	65
5.2 Proposed Design Procedure	66
5.3 Illustrative Examples	70
REFERENCES	77
APPENDIX A - SAMPLE INPUT DATA AND RESULTS	79
APPENDIX B - COMPARISON OF ANALYTICAL AND EXPERIMENTAL RESTRAINT FORCES FOR PROTOTYPE TESTS	83
APPENDIX C - COMPARISON OF ANALYTICAL AND EXPERIMENTAL RESTRAINT FORCES FOR QUARTER SCALE MODEL TESTS	91

LIST OF FIGURES

Figure	Page
1.1 Purlin Cross-Section and Geometric Parameters	2
1.2 Partial Restraint of Purlins	5
1.3 Needham's Mathematical Model	5
1.4 Ghazanfari's Mathematical Model	8
2.1 Actual System with Torsional Restraint . . .	13
2.2 Actual System with Third Points Restraint . .	13
2.3 Actual System with Midspan Restraint	13
2.4 System Stiffness Model	15
2.5 Purlin Stiffness Model	17
2.6 Panel Stiffness Model	18
2.7 Purlin Cross-Section	21
2.8 Applied Purlin Load	22
3.1 Typical Prototype and Model Cross Section . .	26
3.2 Typical Test Setup Cross Section	26
4.1 Purlin Lip Detail	38
4.2 Variation of Percent Brace Force with Number of Purlin Lines	42
4.3 Variation of Percent Brace Force with Span Length	43

4.4	Variation of Percent Brace Force with Purlin Depth	47
4.5	Variation of Percent Brace Force with Purlin Flange Width	47
4.6	Variation of Percent Brace Force with Purlin Thickness	47
4.7	Variation of Percent Brace Force with Number of Spans	49
4.8	Brace Force Distributions for Multiple Span Systems	51
4.9	Variation of Percent Brace Force with Roof Slope	52
4.10	Natural Logarithm of Percent Brace Force Versus Number of Purlin Lines	56
4.11	Predicted versus Theoretical Percent Brace Force for Single Span Systems	60
4.12	Predicted versus Theoretical Percent Brace Force for Three Span Systems	61
4.13	Predicted and Theoretical Variation of Percent Brace Force with Number of Purlin Lines	62
4.14	Predicted and Theoretical Variation of Percent Brace Force with Purlin Depth	62
4.15	Predicted and Theoretical Variation of Percent Brace Force with Purlin Flange Width	63
4.16	Predicted and Theoretical Variation of Percent Brace Force with Purlin Thickness . .	63
5.1	Brace Force Distribution for Example 4 . . .	75
A.1	Cross Section and Parameter Specification . .	80
A.2	Joint and Member Numbering and Member Properties	81
B.1	Experimental and Analytical Results for Test A/2-3 from Reference [6]	84
B.2	Experimental and Analytical Results for Test A/7-2 from Reference [6]	85

B.3	Experimental and Analytical Results for Test 3A/2-1	86
B.4	Experimental and Analytical Results for Test B/2-1-A from Reference [6]	88
B.5	Experimental and Analytical Results for Test B/6-3	89
B.6	Experimental and Analytical Results for Test III from Reference [5]	90
C.1	Experimental and Analytical Results for Test C/2-1 from Reference [7]	92
C.2	Experimental and Analytical Results for Test C/6-1 from Reference [7]	93
C.3	Experimental and Analytical Results for Test C/2-15 from Reference [7]	94
C.4	Experimental and Analytical Results for Test C/2-10 from Reference [7]	95
C.5	Experimental and Analytical Results for Test C/6-2 from Reference [7]	96
C.6	Experimental and Analytical Results for Test C/6-3 from Reference [7]	97
C.7	Experimental and Analytical Results for Test 3C/2-1 from Reference [7]	98
C.8	Experimental and Analytical Results for Test 3C/2-4 from Reference [7]	100
C.9	Experimental and Analytical Results for Test 3C/2-3 from Reference [7]	102
C.10	Experimental and Analytical Results for Test S1/2-15	104
C.11	Experimental and Analytical Results for Test S1/2-25	105
C.12	Experimental and Analytical Results for Test S4/2-15	106
C.13	Experimental and Analytical Results for Test S4/2-25	107

LIST OF TABLES

Table	Page
2.1 Comparison of Analytical Model Results with Experimental Results	24
3.1 Test Series and Configurations	27
4.1 Purlin Cross Sectional Dimensions and Properties Used in the Parametric Study	36
4.2 Flexural Capacities of Purlin Sections Used in the Parametric Study	40
4.3 Ultimate Simple Span Uniformly Distributed Loads . . .	40
4.4 Roof Systems Analyzed to Obtain Data for Regression Analyses Input	54

PREDICTION OF LATERAL RESTRAINT FORCES FOR Z-PURLIN SUPPORTED ROOF SYSTEMS

CHAPTER I

INTRODUCTION AND LITERATURE REVIEW

1.1 Scope

Cold formed, Z-shaped purlins are relatively thin, light weight sections, obtained by bending a steel strip in a press brake or a cold-forming machine. Due to their ease of erection and handling, they are extensively used in the steel building industry as secondary structural members in roofing systems. Because of their unsymmetrical shape, (see Figure 1.1), Z-purlins are loaded obliquely to their principal axes when the line of action of the applied load is in the plane of the web, thus, they tend to deflect perpendicular to, as well as, in the plane of the loading. In addition, if the loads are applied eccentrically or if the purlin is restrained at only one flange, torsional moments are induced causing the purlin to twist around its longitudinal axis. The combination of lateral movement and twisting is known to be detrimental to the load carrying capacity of the member.

In most practical cases, a roof panel is attached to the top flange of each purlin throughout its length. This panel usually provides enough stiffness to prevent the relative movement of the purlins with respect to each

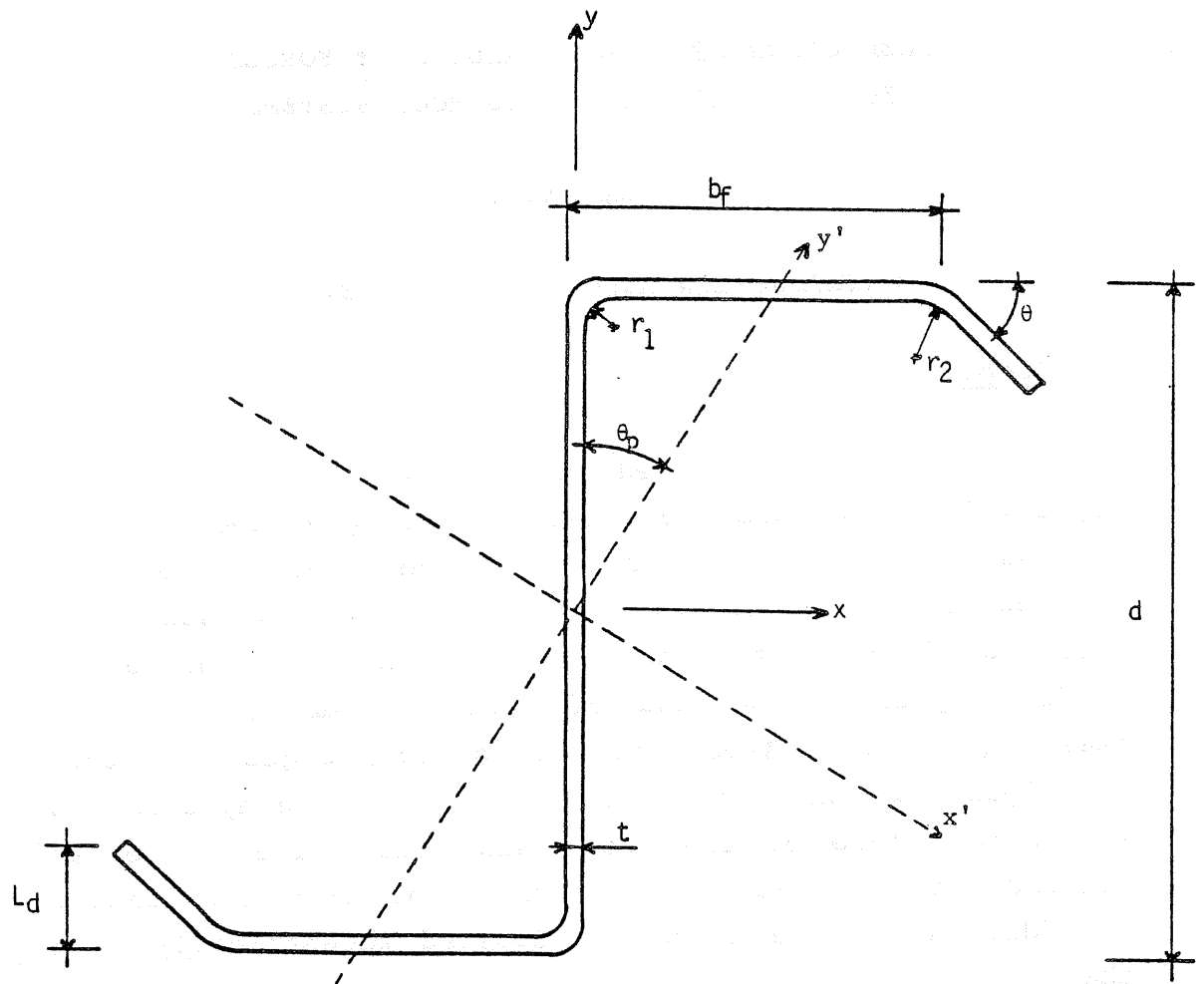


Figure 1.1 Purlin Cross-Section and Geometric Parameters

other, but, unless an external restraint is provided, the system as a whole will tend to move laterally. This restraint usually consists of discrete members called "braces" attached to the purlin at discrete locations along the span and designed to carry forces induced from restraining the system against lateral movement. The determination of the magnitude of such forces has been studied by several researchers, however, methods to accurately predict these forces in multiple span, multiple purlin line systems are not currently available. The purpose of this study is to develop an analytical model to predict restraint forces in thru fastener, multiple span, multiple purlin line, Z-purlin supported roof systems.

1.2 Review of Previous Research

Zetlin and Winter [1] studied the case of a single-span simply supported Z-purlin, subjected to concentrated and uniform loads applied in the plane of its web. The purlin is assumed to be laterally braced at both flanges at all load locations for the case of applied concentrated loads and continuously when the load is uniformly distributed. Zetlin and Winter found that the forces acting on these braces vary linearly with the applied loads and can be determined from

$$BF_x = (I_{xy}/I_x) W_y \quad (1.1)$$

where BF_x is the brace force to be determined, I_{xy} is the moment product of inertia of the purlin cross-section about the axes parallel and perpendicular to the web, I_x is the moment of inertia of the purlin cross-section about an axis perpendicular to the web and W_y is the applied load. Equation 1.1 forms the basis of the brace force

requirements in the American Iron and Steel Institute "Specifications for the Design of Cold-Formed Members" [2], which will henceforth be referred to as the Specification. The brace forces predicted by Equation 1.1 usually range between 25 and 40% of the total applied load.

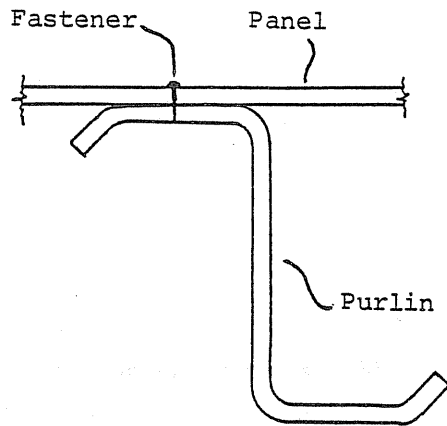
In practice, Z-purlins are usually attached to a roofing panel at their top flange. The shear and torsional stiffnesses of this panel provide partial restraint to the purlin as shown in Figure 1.2. Needham [3] has suggested a mathematical model that enables one to determine the forces in the attached panel. His model is based on the assumptions that: (1) The purlin is simply supported; (2) no lateral bracing is connected directly to the purlins; (3) the panel diaphragm is infinitely rigid; and (4) the diaphragm is prevented from moving laterally with respect to the purlins. Referring to Figure 1.3, the cross-section is subjected to a torque T_w caused by the vertical load W assumed to be applied at an eccentricity e measured from the web of the purlin. Needham suggested that e should be taken equal to $b_f/6$, where b_f is the flange width. In addition, since the restraint force W_p provided by the panel is applied to the top flange at a distance $d/2$ from the shear center, where d is the total depth of the purlin, another torque T_p is generated. The total torque acting on the cross-section is then

$$T = T_w + T_p = W e - W_p (d/2) \quad (1.2)$$

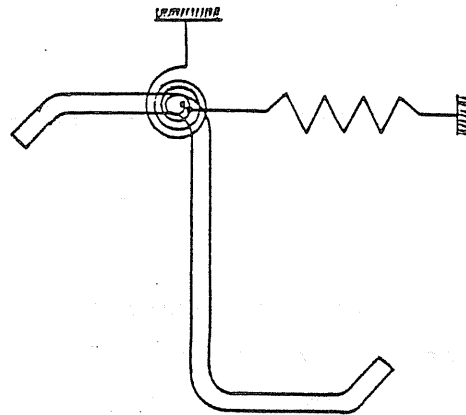
which, upon substitution of $e = b_f/6$, becomes

$$T = W(b_f/6) - W_p (d/2) \quad (1.3)$$

Needham [3] assumed that $W_p = W(I_{xy}/I_x)$. It follows

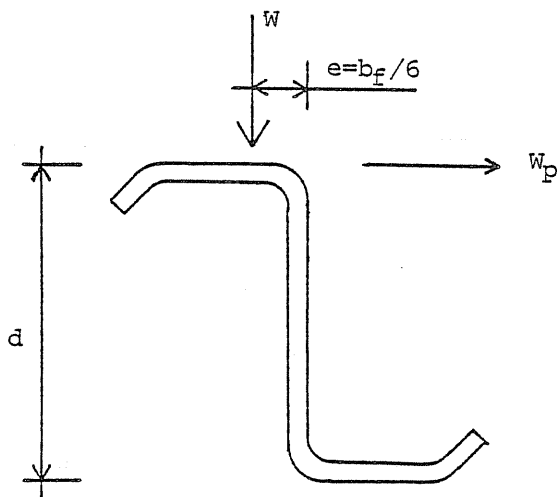


a) Actual System

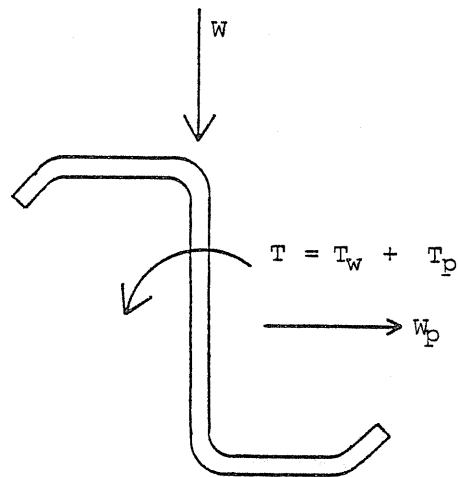


b) Model

Figure 1.2 Partial Restraint of Purlins



a) Applied Load



b) Resultant Forces

Figure 1.3 Needham's Mathematical Model

then that the total torque is

$$T = W [(b_f/6) - (I_{xy}/I_x)(d/2)] \quad (1.4)$$

For the cross-section to be in equilibrium and for the zero rotation condition to be satisfied, a resisting torque must be provided all along the span. This can be accomplished by introducing a lateral secondary force W_{ps} , applied to the panel at a distance $d/2$ from the shear center. Equilibrium requires that

$$W_{ps} = T / (d/2) \quad (1.5)$$

which can be written as

$$W_{ps} = W [(b_f/3d) - (I_{xy}/I_x)] \quad (1.6)$$

The total net force at the panel, which is also the required lateral restraint force, is then

$$W_{net} = W [(I_{xy}/I_x) \cos \theta - \sin \theta] + W_{ps} \quad (1.7)$$

where θ is the angle of the roof with the horizontal.

Needham states that laboratory tests have shown that this method gives acceptable results depending on the value chosen for the eccentricity of the vertical load. One sixth of the flange width is apparently not always adequate.

Ghazanfari and Murray [4] considered single, simple-span Z-purlins subjected to uniform gravity loading and various bracing configurations. The mathematical model they used assumed: (1) zero panel rotational restraint;

(2) no slip between the purlin and the panel at the fastener locations; (3) the line of action of the vertical uniform load W_v is located at the third of the flange from the plane of the web; (4) the lateral panel force w_h is uniformly distributed and acts at the connection of the web to the compression flange in a plane perpendicular to the web; and (5) the lateral braces are connected to a rigid eave and are infinitely rigid themselves. Figure 1.4 shows the model.

In this model, the purlin lateral and vertical deflections are caused due to the presence of forces W_v and W_h . Since these forces are not applied at the shear center of the section, they will produce a torque that tends to increase the lateral movement of the top flange. On the other hand, the panel deformation will tend to reduce that primary torque. Since the panel deformation cannot be determined unless the lateral force W_h is known, which also cannot be calculated unless the total torque is known, an iterative procedure is required to solve the problem. Ghazanfari and Murray developed a computer program that determines the lateral force W_h including second order effects. The procedure is as follows:

- Step 1 Assume zero second order effects.
- Step 2 Calculate the lateral force W_h .
- Step 3 Calculate the diaphragm deflection.
- Step 4 Revise the value of the torque by introducing secondary effects due to the panel deformation.
- Step 5 Recalculate W_h .
- Step 6 Compare with previous cycle and repeat steps 3 to 5 until convergence is attained.

Full-scale tests were conducted to verify the adequacy

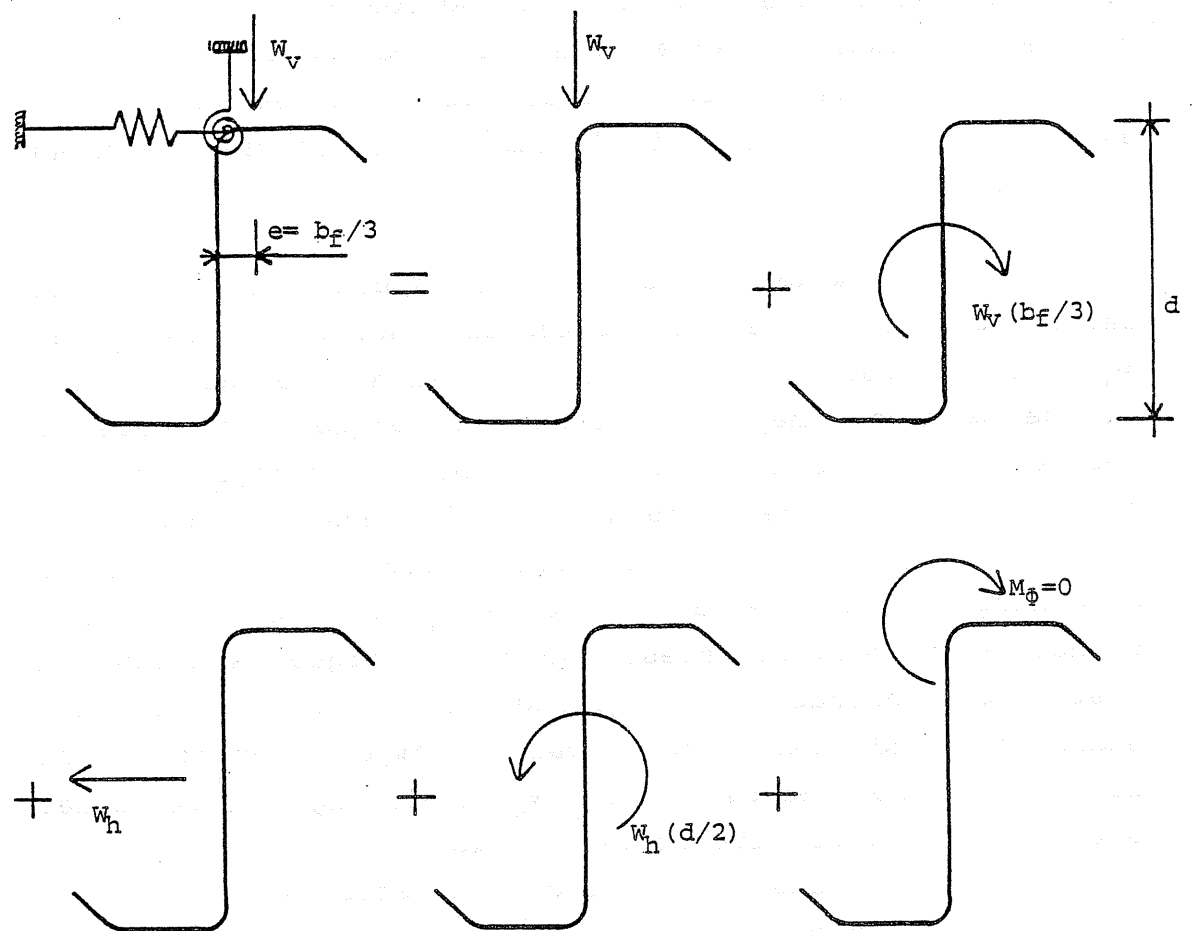


Figure 1.4 Ghazanfari's Mathematical Model

of this analytical method [5]. The analytical and experimental results were found to be in good agreement. The total brace force was found to vary from 14% to 29% of the total applied vertical load depending on the span and lateral brace configuration.

Curtis and Murray [6] reported the results of a series of tests that were conducted to study the accumulation of lateral forces when the number of purlin lines is increased. Tests were conducted using roof systems supported by 2, 4 and 6 purlin lines. It was found that the ratio of the lateral forces to the total applied vertical load decreases by up to 60% with an increasing number of purlin lines. The same conclusions were drawn from the results of tests conducted by Seshappa [7], who used cold-formed quarter-size Z-purlins to study the lateral restraint requirements for Z-purlin supported roof systems. Seshappa conducted 28 quarter scale tests, using single span and three continuous span configurations with 2 and 6 purlin lines and different bracing configurations. Some of tests were conducted to study the effect of roof slope on brace forces. The tests conducted by Seshappa were in very good agreement with prototype tests that were conducted earlier, especially for the variation of lateral restraint with number of purlin lines.

Thus, it is evident that the aforementioned methods of analysis cannot be applied to multiple purlins systems. A conservative approach is to assume that every purlin is braced individually and that the total restraint force required for a system is equal to the force required for a single purlin line multiplied by the number of purlin lines.

1.3 Current Design Practice

Provisions to determine the required lateral restraint forces for Z-purlins supported roof systems are recommended in the American Iron and Steel Institute "Specification for the Design of Cold-Formed Members" [2]. These provisions state that bracing is not required if both of the purlin's flanges are attached to a sheeting material. However, if only one flange is connected, then, the brace shall be designed to resist a lateral force $P_1 = 1.5(I_{xy}/I_x)$ times the load within a distance $0.5a$ each side of the brace, where "a" is the length of bracing interval. Slightly different provisions are recommended for the case where the purlin is not attached to a panel.

However, it is known that a number of metal building manufacturers do not provide lateral restraint other than that provided by the pan and eave strut or ridge members. Others use opposed purlin configurations and/or shear plates at the rafters.

1.4 Conclusions and Justification of Study

It is well known that the capacity of a roofing system is considerably increased when an adequate lateral bracing is provided. The effectiveness of a brace depends strongly on the way it is designed. Several approaches of determining the lateral forces a brace is required to carry were discussed in the beginning of this Chapter. The approach proposed by Ghazanfari and Murray [3] was found to be in good agreement with single-span, two purlin line test results, but is too conservative for multiple purlin line systems.

The objective of this study is to develop an adequate design approach for bracing requirements of single or multiple span, multiple Z-purlin line systems with different bracing configurations. For this purpose, a mathematical model is developed in Chapter II and used to study the variation of lateral restraint forces depending on the bracing configuration, purlin dimensions, number of purlin lines and the number of spans. Results are compared to experimental results and are found to be sufficiently accurate for design purposes. Brace force design equations are then developed using regression analysis and design examples are given at the end of this thesis.

CHAPTER II

DEVELOPMENT OF A MATHEMATICAL MODEL

2.1 Overview

A metal building roofing system is a combination of three types of structural elements: purlins for strength, a panel or deck for serviceability and external restraint braces for stability. The Z-shaped purlins are usually attached to the main framing of the structure at their bottom flange and to a corrugated steel panel at their top flange, as shown in Figure 2.1. Ordinary mild steel bolts are used for the purlin-to-rafter connections and self-drilling fasteners are usually used for the panel-to-purlin connections.

The restraint braces are intended to limit the lateral displacements of the system. They are usually attached to the web of the purlin, near the top flange. For practical reasons, these braces are not provided continuously along the span - an ideal situation - but are located at discrete locations chosen by the designer. In this particular study, three bracing configurations are considered, which are defined as follows:

1. Torsional Restraint (Figure 2.1): In this configuration the braces are located at the rafters and provide a torsional simple support condition at the ends of

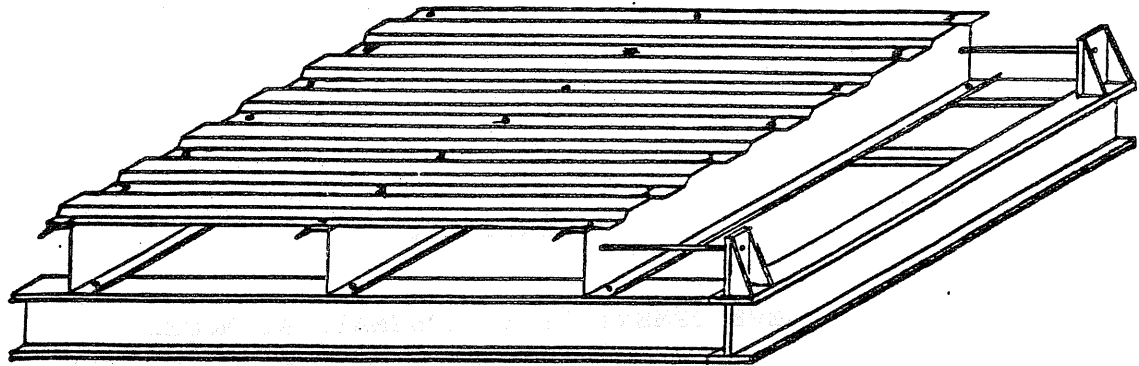


Figure 2.1 Actual System With Torsional Restraint

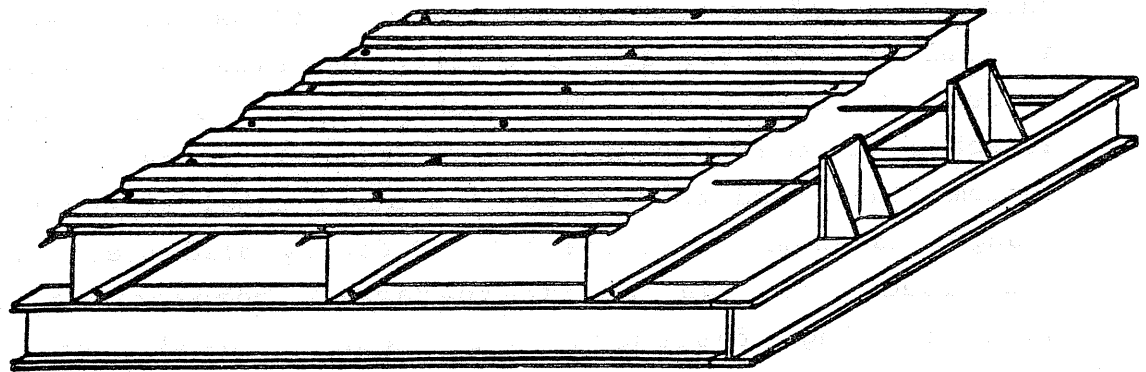


Figure 2.2 Actual System With Third Point Restraint

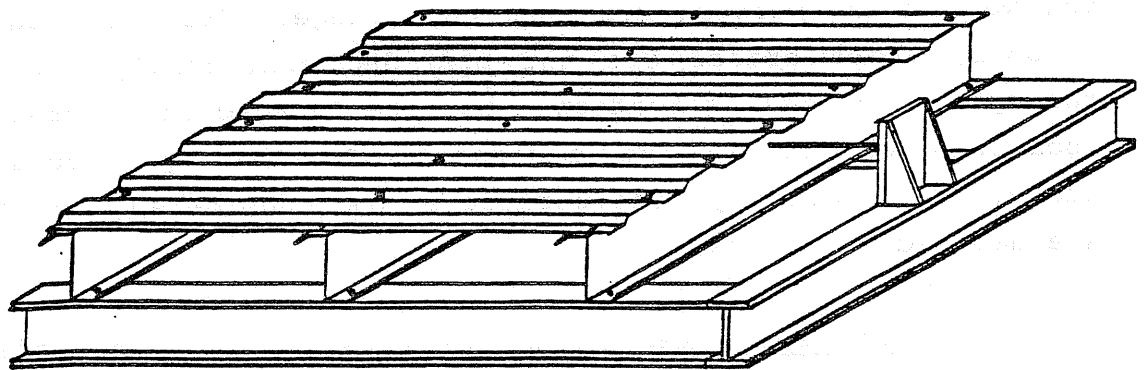


Figure 2.3 Actual System With Mid-span Restraint

the braced purlin.

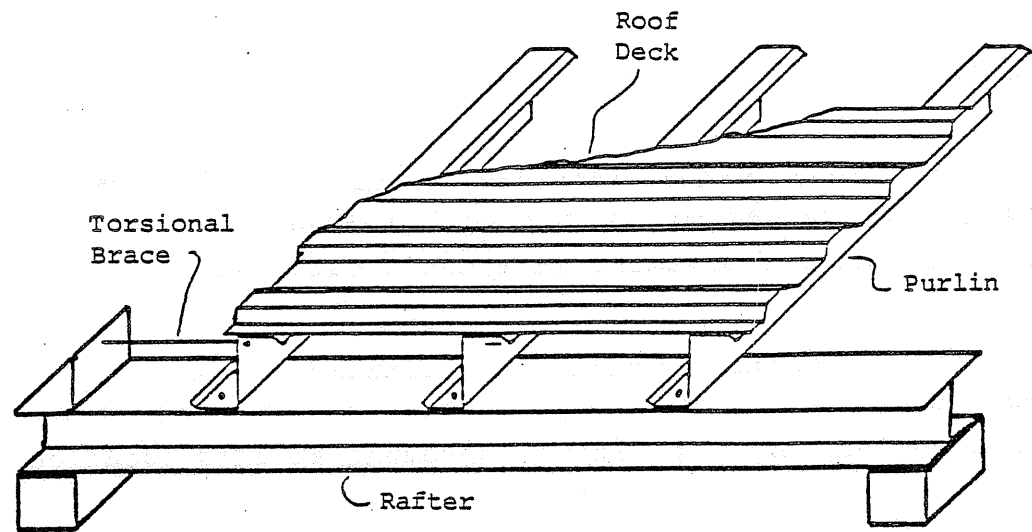
2. Third Point Restraint (Figure 2.2): Here, the braces are connected to the purlin span third points and restrain lateral movement at these locations.

3. Mid-span Restraint (Figure 2.3): In this configuration, braces are connected to the purlin at its mid-span and restrain lateral movement at this location.

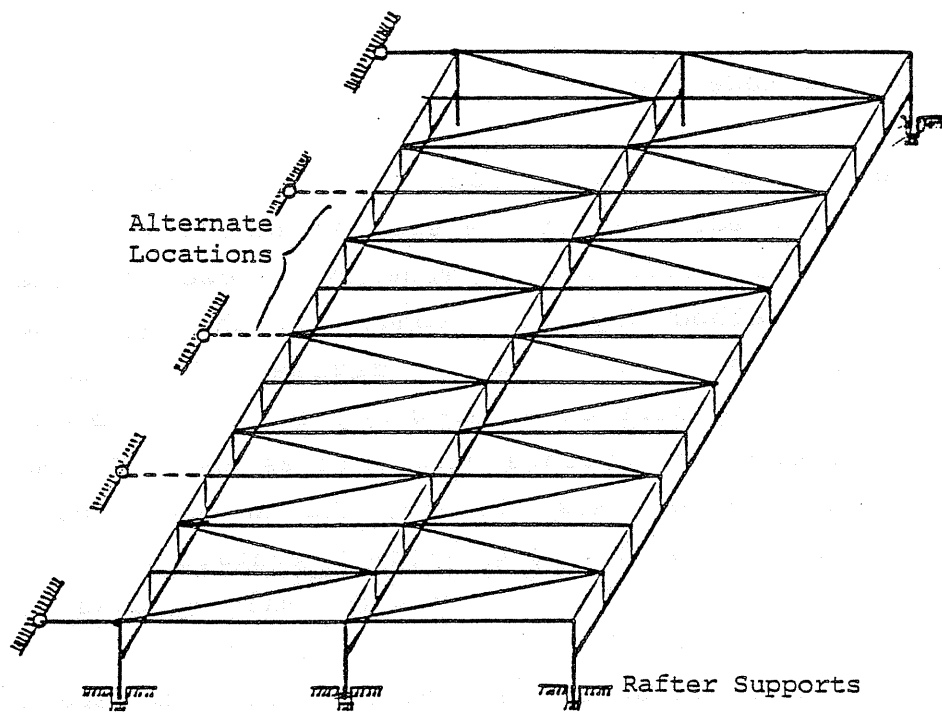
A mathematical model to be used to predict the magnitude of force each of the configurations is now developed.

2.2 Mathematical Modeling

The model chosen should be consistent with the method of analysis to be used. The finite element analysis method is appropriate for roof system modeling, however, the accuracy of this method depends strongly on the type and number of elements used. Twelve-degree of freedom plate elements provide sufficient accuracy for the problem, but the required computer storage capabilities and CPU time would be extremely large. Most likely, the analysis would not be economically feasible for systems containing more than three or four purlin lines. Since the main purpose of the analysis is to calculate external restraint forces rather than internal stresses, a hybrid space frame/space truss model was developed. Figure 2.4 illustrates the proposed mathematical model, which will be referred to as "the stiffness model" for the remainder of this thesis. The three main components of the system, purlin, panel and brace, are first considered separately then combined to develop the whole system model. The stiffness method is



a) Actual System



b) Stiffness Model

Figure 2.4 System Stiffness Model

used to obtain results.

2.2.1 Modeling of the Purlin

The purlin is modeled using a space frame line element, referred to here as a Type A element. The purlin is divided into twelve sub-members of equal length as shown in Figure 2.5. The area and inertia properties assigned to these elements are the same as the purlin's cross-sectional properties except for the torsional constant which will be discussed further in this Chapter.

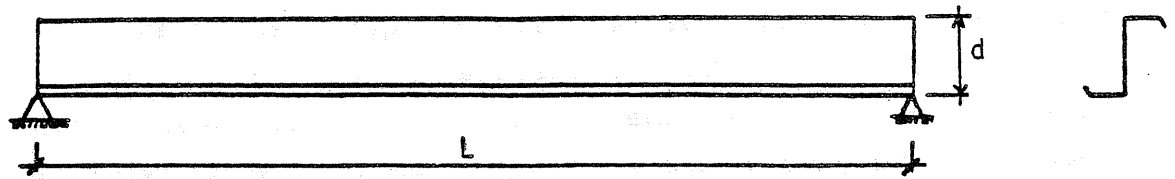
The Type B line elements, shown in Figure 2.5, are provided to satisfy the compatibility of displacements between the purlin and the panel and rafter. The required cross-sectional properties of these elements were adjusted by trial and error to obtain good correlation with prototype and model test results.

2.2.2 Modeling of the Panel

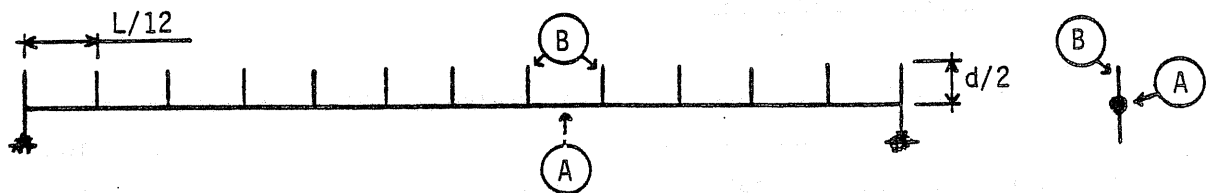
Assuming that the purlin-to-panel connection does not provide rotational restraint to the purlin, the panel bending stiffness can be disregarded and only its shear stiffness need be considered. Since the panel is a planar structure, it can easily be represented by a plane truss.

For a known shear stiffness G' , the deflection of a shear panel in the direction of the load P in Figure 2.6(a) can be determined from [8]

$$\Delta = (P L) / (4 G' a) \quad (2.1)$$

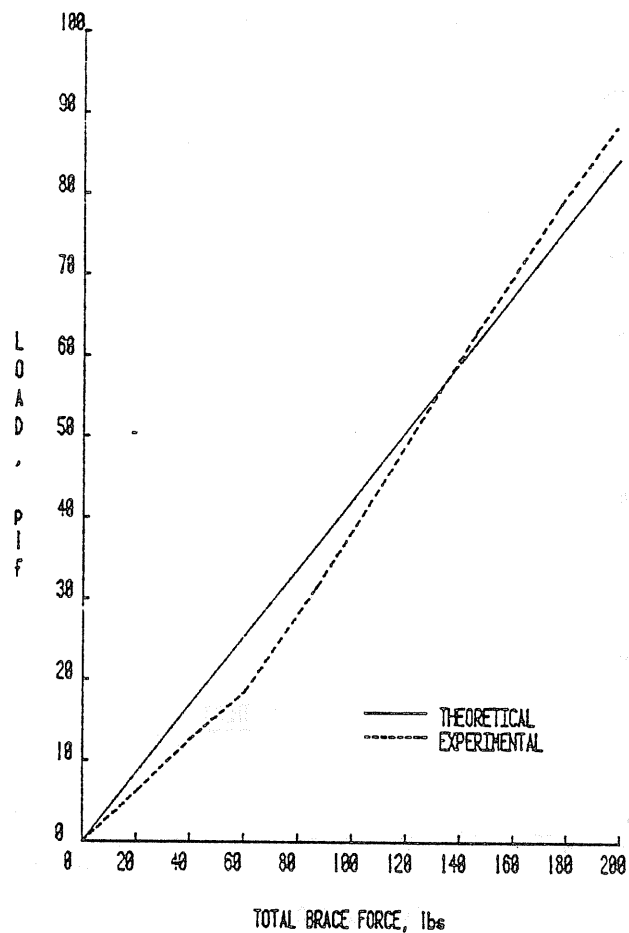


a) Actual System



b) Stiffness Model

Figure 2.5 Purlin Stiffness Model

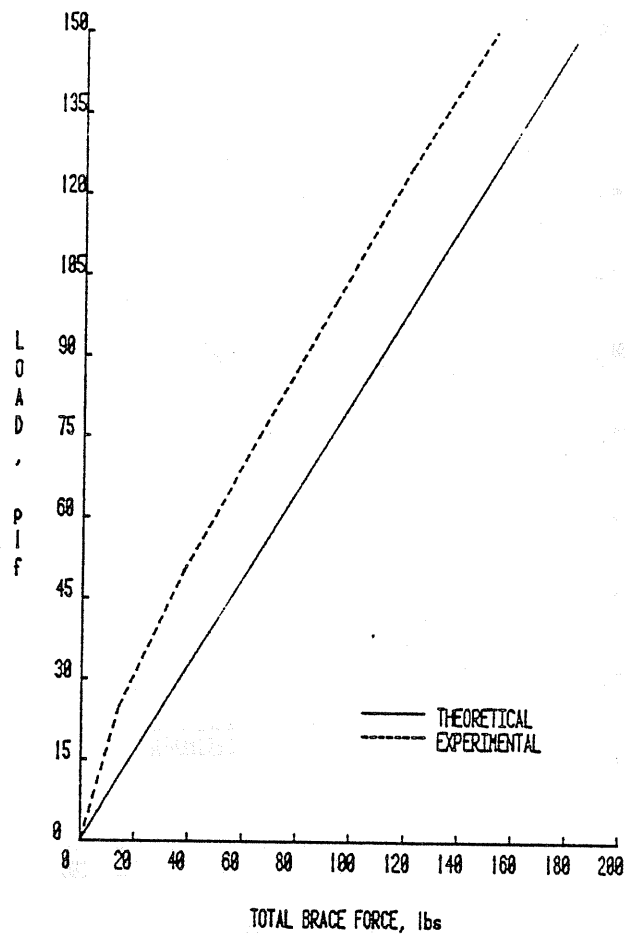


a) Applied Load versus Total Brace Force

Type	: Quarter Scale
Span(s)	: 3
Span Length	: 6.25 ft.
Restraint Configuration	: Torsional
Purlin Lines	: 2
Purlin Depth	: 1.5 in.
Material Thickness	: 0.025 in.

b) Test Parameters

Figure C.13 Experimental and Analytical Results for
Test S4/2-25

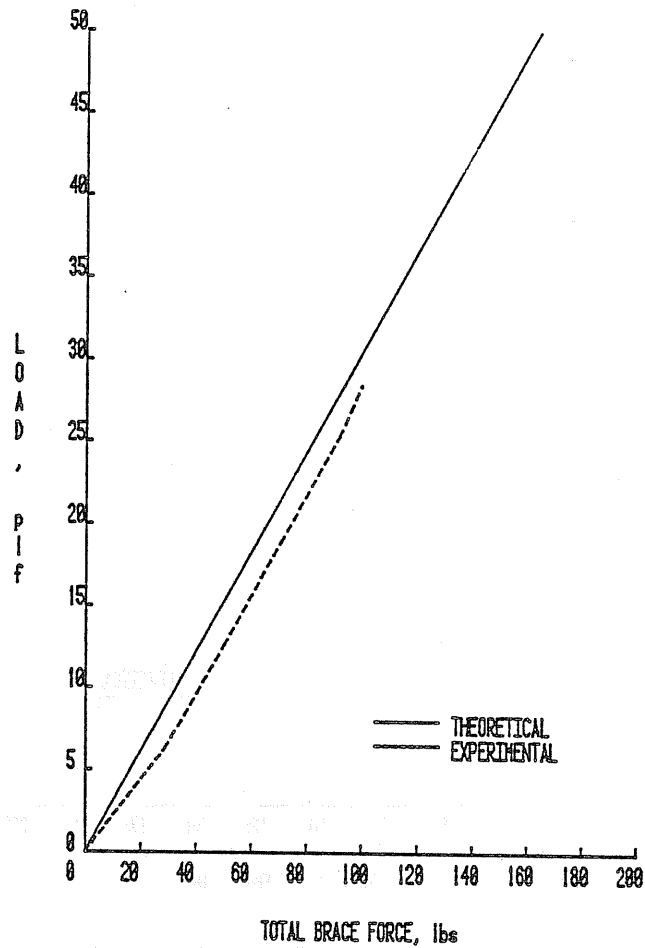


a) Applied Load versus Total Brace Force

Type	: Quarter Scale
Span(s)	: 3
Span Length	: 3.75 ft.
Restraint Configuration	: Torsional
Purlin Lines	: 2
Purlin Depth	: 1.5 in.
Material Thickness	: 0.025 in.

b) Test Parameters

Figure C.12 Experimental and Analytical Results for
Test S4/2-15

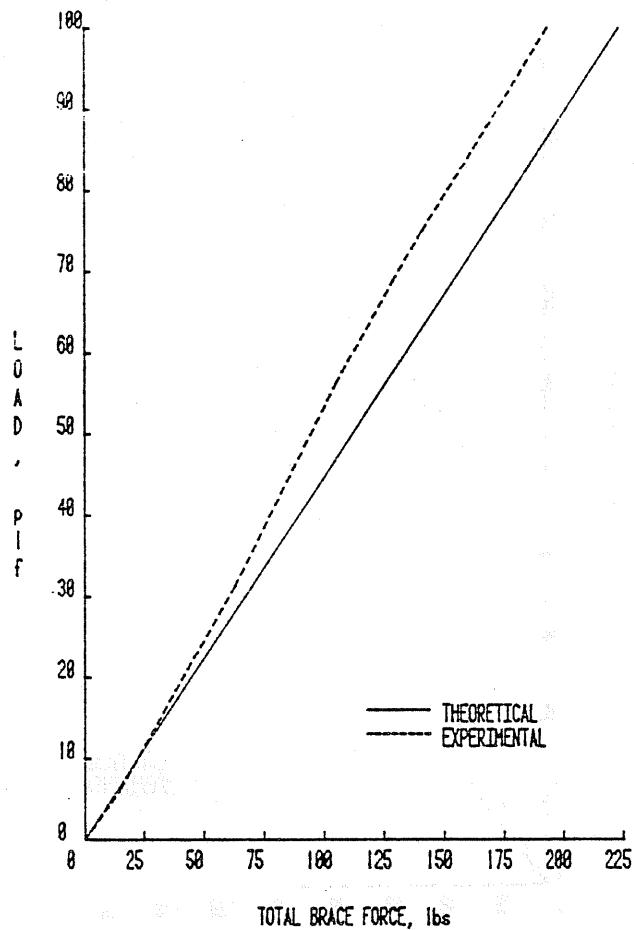


a) Applied Load versus Total Brace Force

Type	: Quarter Scale
Span(s)	: 3
Span Length	: 6.25 ft.
Restraint Configuration	: Torsional
Purlin Lines	: 2
Purlin Depth	: 1.5 in.
Material Thickness	: 0.025 in.

b) Test Parameters

Figure C.11 Experimental and Analytical Results for
Test S1/2-25

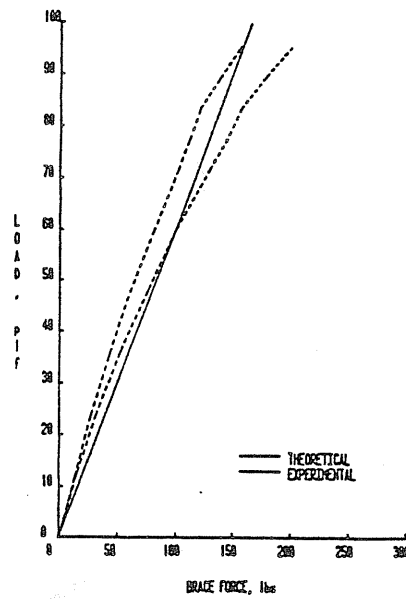


a) Applied Load versus Total Brace Force

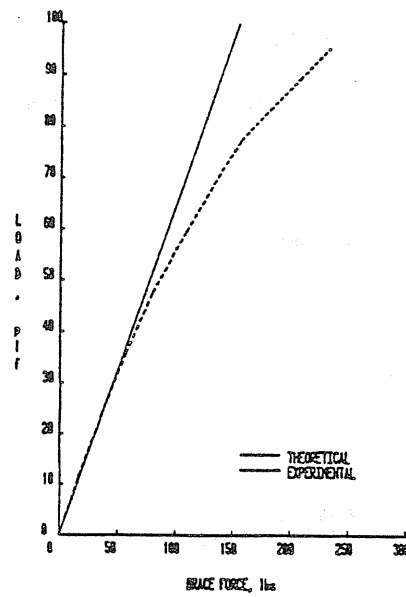
Type	: Quarter Scale
Span(s)	: 1
Span Length	: 3.75 ft.
Restraint Configuration	: Torsional
Purlin Lines	: 2
Purlin Depth	: 1.5 in.
Material Thickness	: 0.025 in.

b) Test Parameters

Figure C.10 Experimental and Analytical Results for
Test S1/2-15

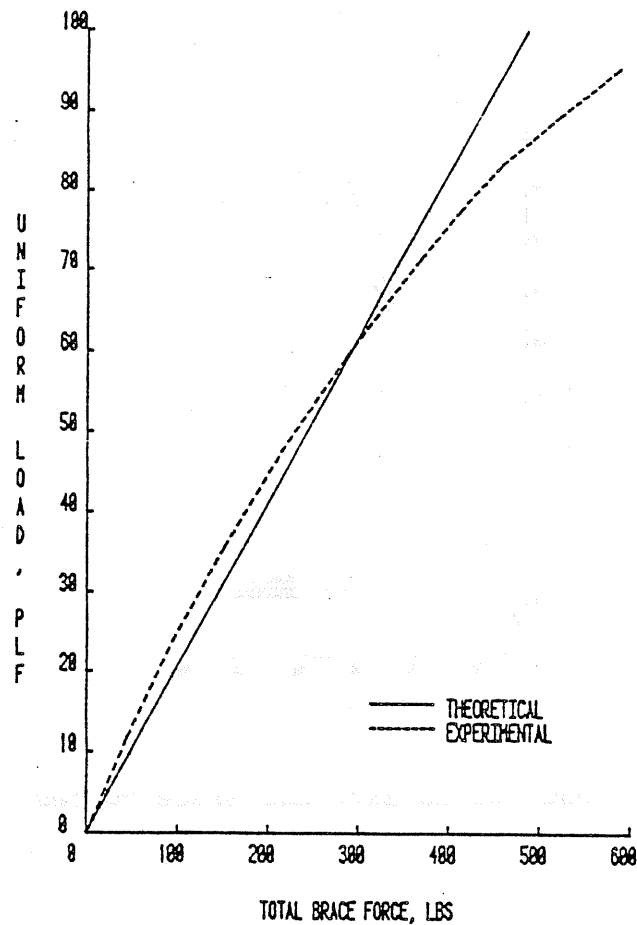


c) Applied Load versus External Brace Forces



d) Applied Load versus Internal Brace Forces

Figure C.9 Experimental and Analytical Results for Test 3C/2-3 from Reference [7], continued

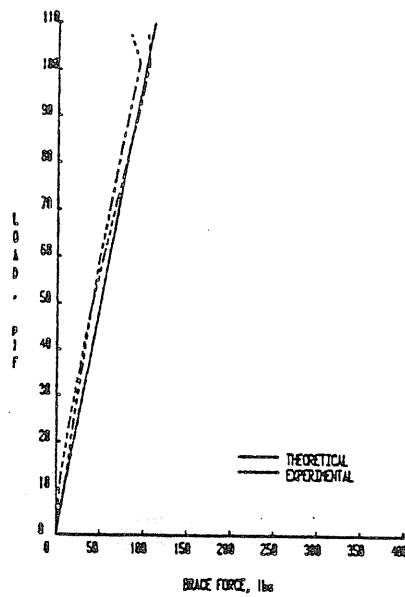


a) Applied Load versus Total Brace Force

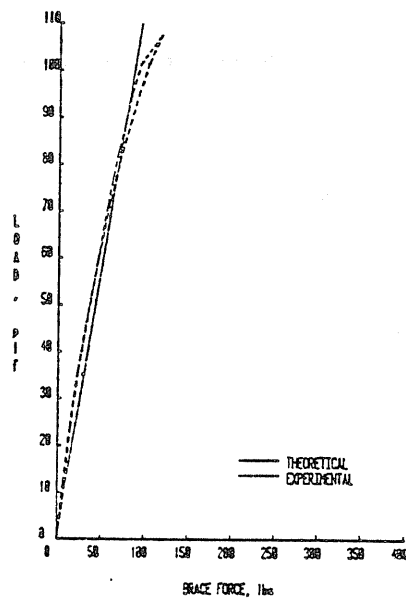
Type	: Quarter Scale
Span(s)	: 3
Span Length	: 5.0 ft.
Restraint Configuration	: Midspan
Purlin Lines	: 2
Purlin Depth	: 2.0 in.
Material Thickness	: 0.025 in.

b) Test Parameters

Figure C.9 Experimental and Analytical Results for
Test 3C/2-3 from Reference [7]

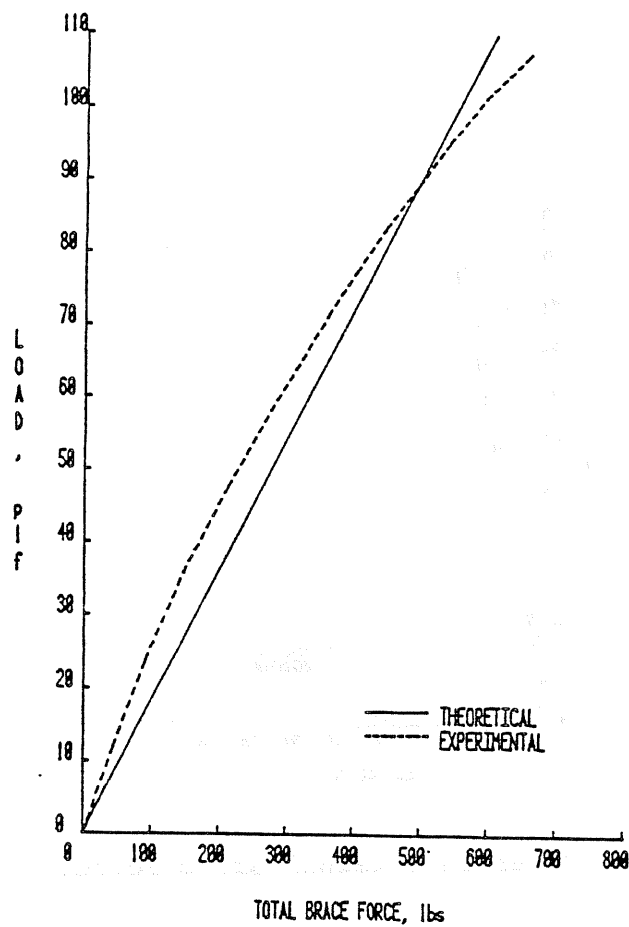


c) Applied Load versus External Brace Forces



d) Applied Load versus Internal Brace Forces

Figure C.8 Experimental and Analytical Results for
Test 3C/2-4 from Reference [7], continued

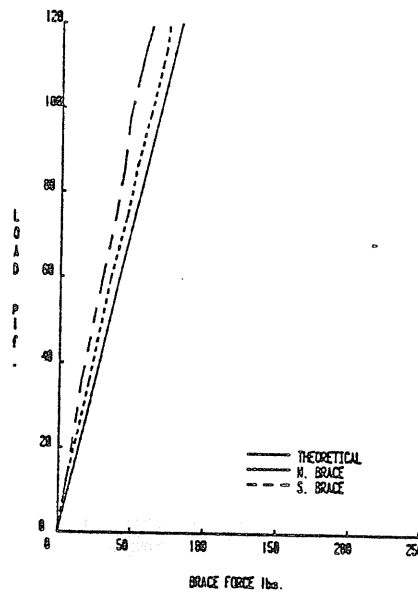


a) Applied Load versus Total Brace Force

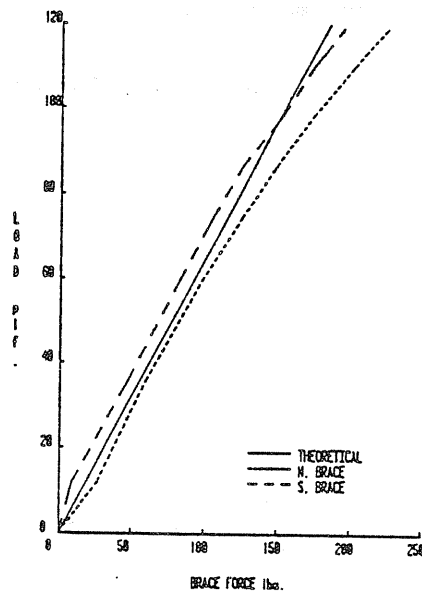
Type	: Quarter Scale
Span(s)	: 3
Span Length	: 5.0 ft.
Restraint Configuration	: Third Point
Purlin Lines	: 2
Purlin Depth	: 2.0 in.
Material Thickness	: 0.025 in.

b) Test Parameters

Figure C.8 Experimental and Analytical Results for
Test 3C/2-4 from Reference [7]

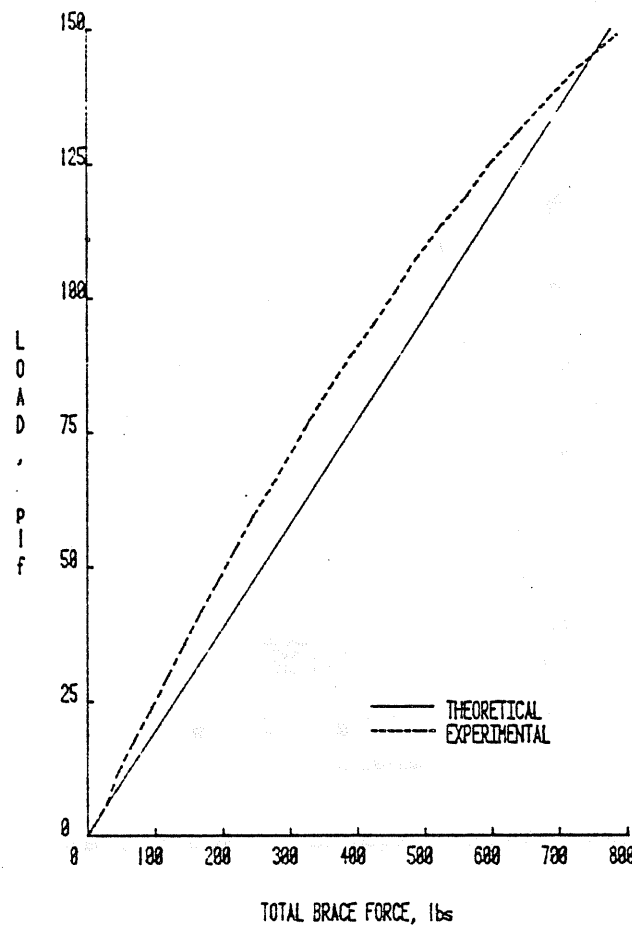


c) Applied Load versus External Brace Forces



d) Applied Load versus Internal Brace Forces

Figure C.7 Experimental and Analytical Results for Test 3C/2-1 from Reference [7], continued

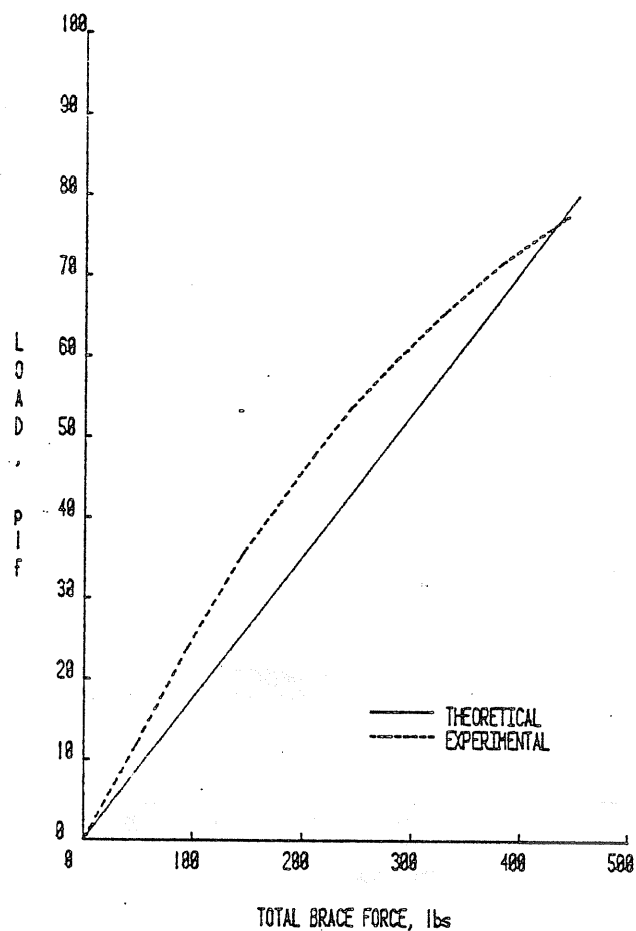


a) Applied Load versus Total Brace Force

Type	: Quarter Scale
Span(s)	: 3
Span Length	: 5.0 ft.
Restraint Configuration	: Torsional
Purlin Lines	: 2
Purlin Depth	: 2.0 in.
Material Thickness	: 0.025 in.

b) Test Parameters

Figure C.7 Experimental and Analytical Results for
Test 3C/2-1 from Reference [7]

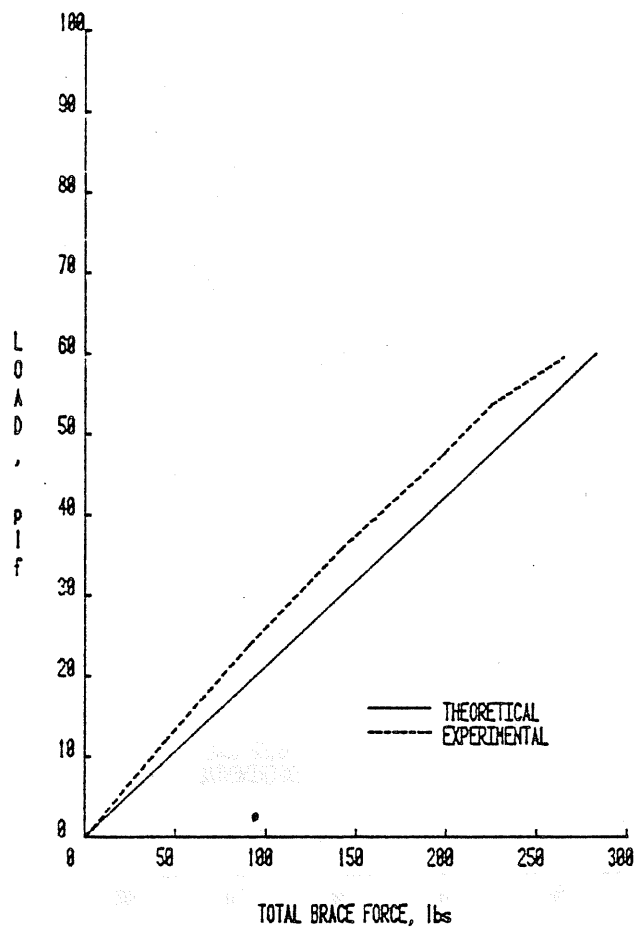


a) Applied Load versus Total Brace Force

Type	: Quarter Scale
Span(s)	: 1
Span Length	: 5.0 ft.
Restraint Configuration	: Midspan
Purlin Lines	: 6
Purlin Depth	: 2.0 in.
Material Thickness	: 0.025 in.

b) Test Parameters

Figure C.6 Experimental and Analytical Results for
Test C/6-3 from Reference [7]

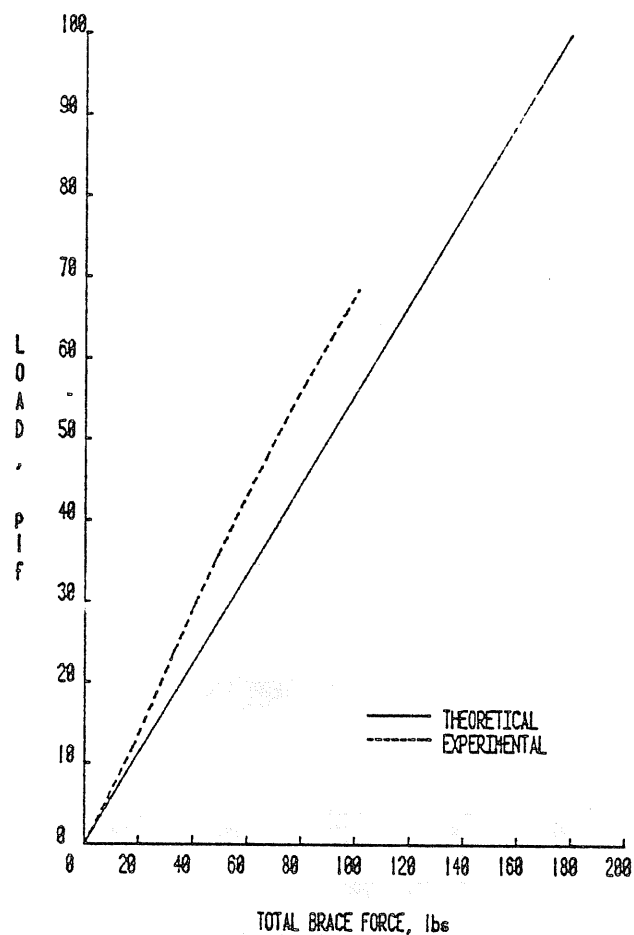


a) Applied Load versus Total Brace Force

Type	: Quarter Scale
Span(s)	: 1
Span Length	: 5.0 ft.
Restraint Configuration	: Third Point
Purlin Lines	: 6
Purlin Depth	: 2.0 in.
Material Thickness	: 0.025 in.

b) Test Parameters

Figure C.5 Experimental and Analytical Results for
Test C/6-2 from Reference [7]

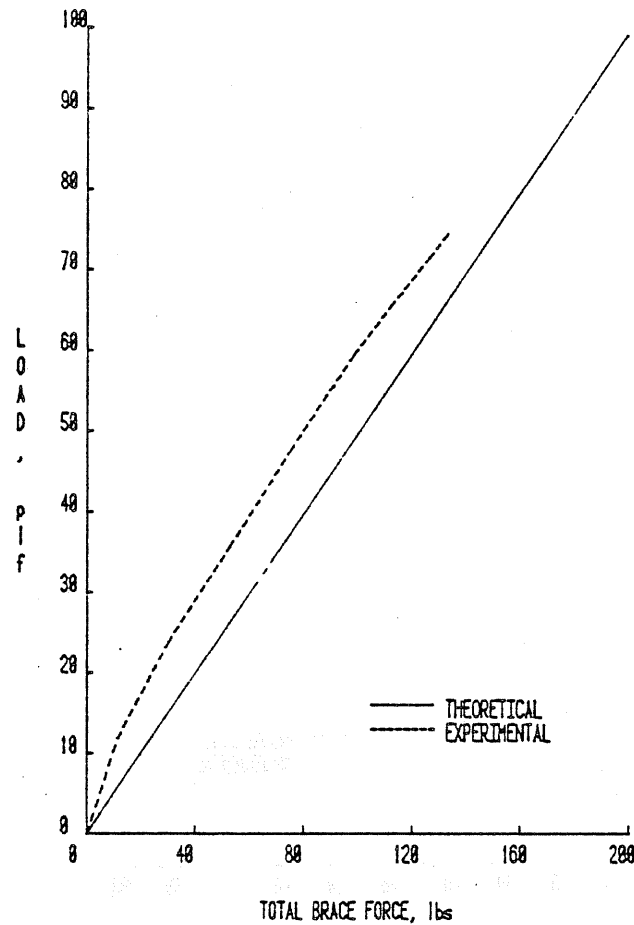


a) Applied Load versus Total Brace Force

Type	: Quarter Scale
Span(s)	: 1
Span Length	: 5.0 ft.
Restraint Configuration	: Midspan
Purlin Lines	: 2
Purlin Depth	: 2.0 in.
Material Thickness	: 0.025 in.

b) Test Parameters

Figure C.4 Experimental and Analytical Results for
Test C/2-10 from Reference [7]

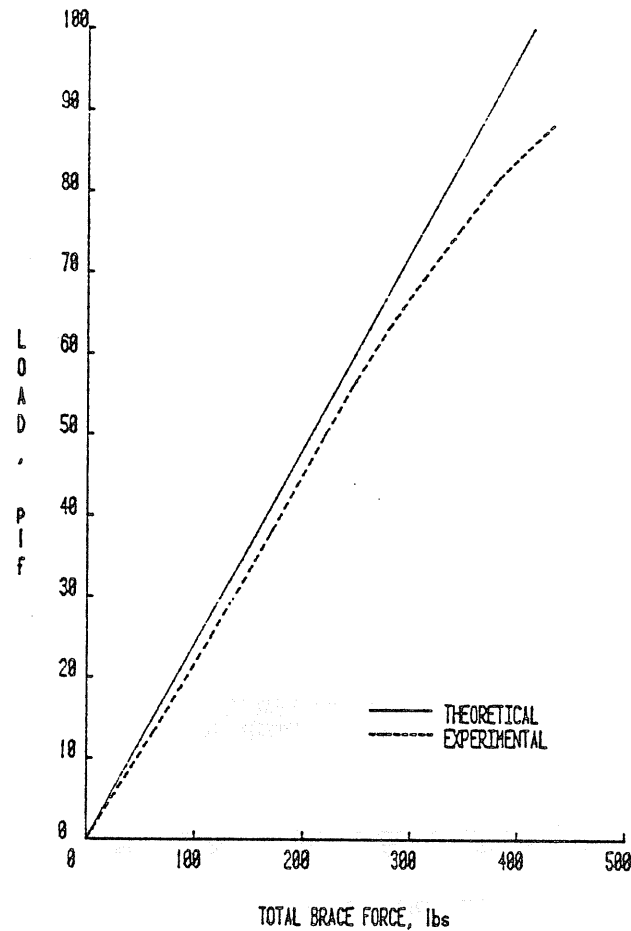


a) Applied Load versus Total Brace Force

Type	: Quarter Scale
Span(s)	: 1
Span Length	: 5.0 ft.
Restraint Configuration	: Third Point
Purlin Lines	: 2
Purlin Depth	: 2.0 in.
Material Thickness	: 0.025 in.

b) Test Parameters

Figure C.3 Experimental and Analytical Results for Test C/2-15 from Reference [7]

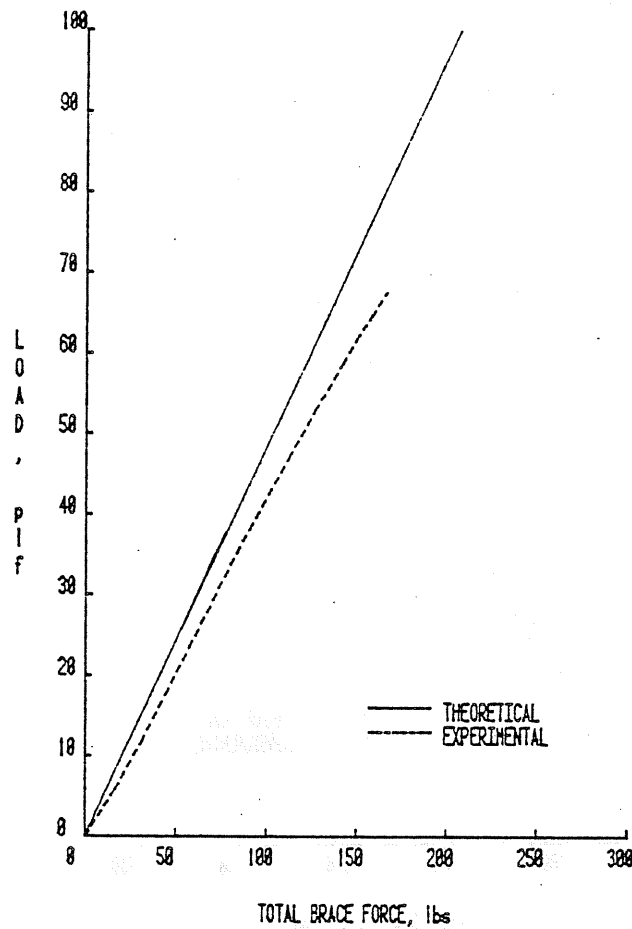


a) Applied Load versus Total Brace Force

Type	: Quarter Scale
Span(s)	: 1
Span Length	: 5.0 ft.
Restraint Configuration	: Torsional
Purlin Lines	: 6
Purlin Depth	: 2.0 in.
Material Thickness	: 0.025 in.

b) Test Parameters

Figure C.2 Experimental and Analytical Results for
Test C/6-1 from Reference [7]



a) Applied Load versus Total Brace Force

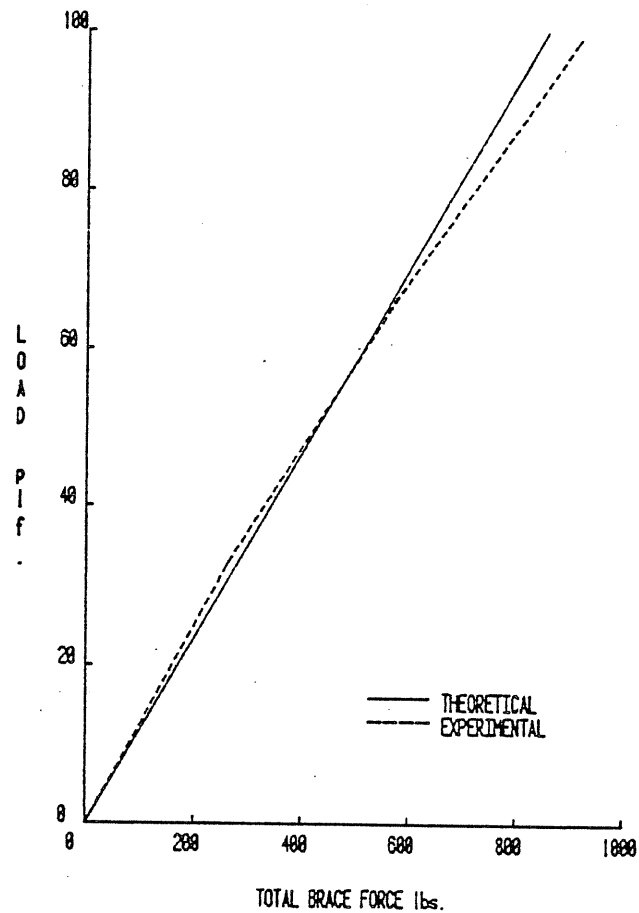
Type	: Quarter Scale
Span(s)	: 1
Span Length	: 5.0 ft.
Restraint Configuration	: Torsional
Purlin Lines	: 2
Purlin Depth	: 2.0 in.
Material Thickness	: 0.025 in.

b) Test Parameters

Figure C.1 Experimental and Analytical Results for
Test C/2-1 from Reference [7]

APPENDIX C

COMPARISON OF ANALYTICAL AND EXPERIMENTAL RESTRAINT FORCES FOR QUARTER SCALE MODEL TESTS

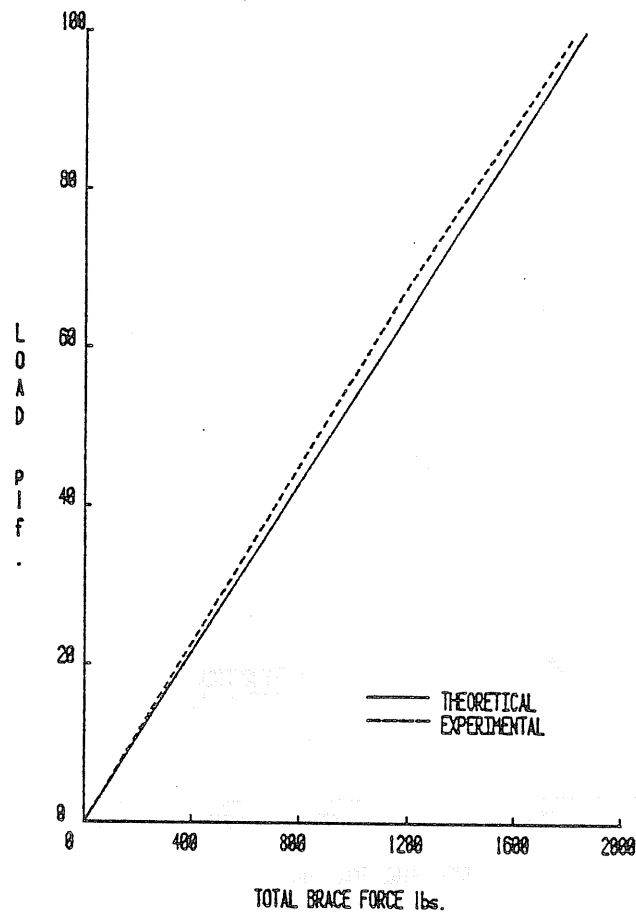


a) Applied Load versus Total Brace Force

Type	: Full Scale
Span(s)	: 1
Span Length	: 20.0 ft.
Restraint Configuration	: Torsional
Purlin Lines	: 2
Purlin Depth	: 8.0 in.
Material Thickness	: 0.090 in.

b) Test Parameters

Figure B.6 Experimental and Analytical Results for Test III from Reference [5]

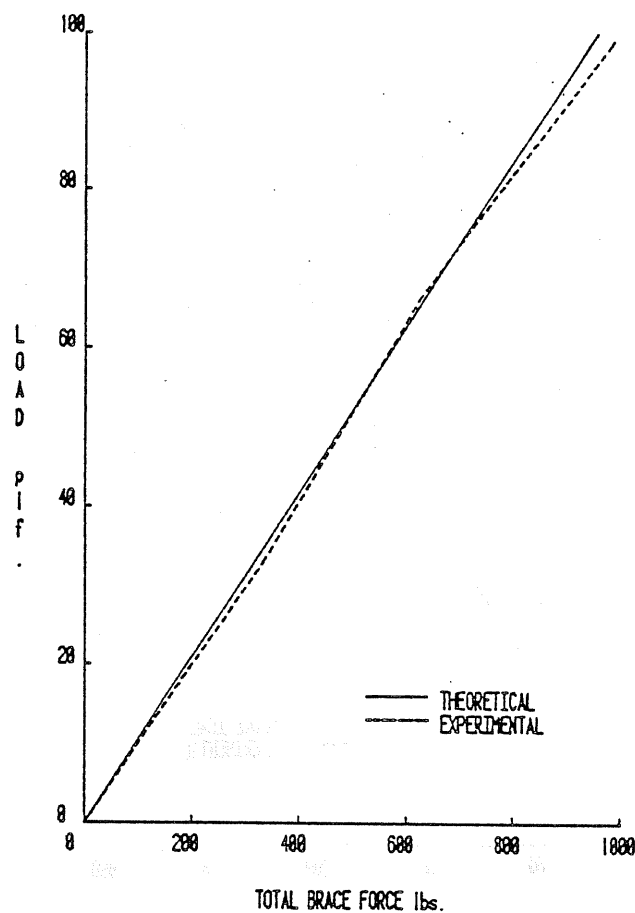


a) Applied Load versus Total Brace Force

Type	: Full Scale
Span(s)	: 1
Span Length	: 22.0 ft.
Restraint Configuration	: Torsional
Purlin Lines	: 6
Purlin Depth	: 8.0 in.
Material Thickness	: 0.090 in.

b) Test Parameters

Figure B.5 Experimental and Analytical Results for
Test B/6-3

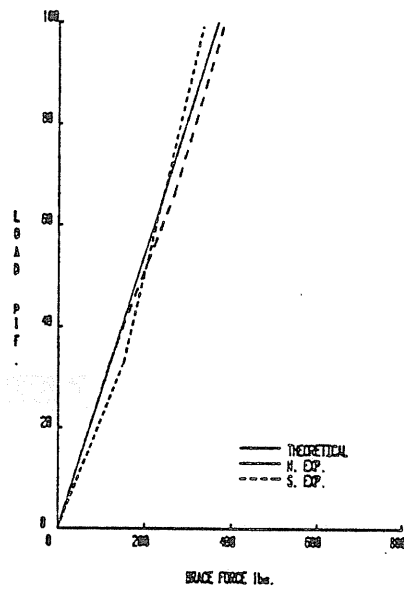


a) Applied Load versus Total Brace Force

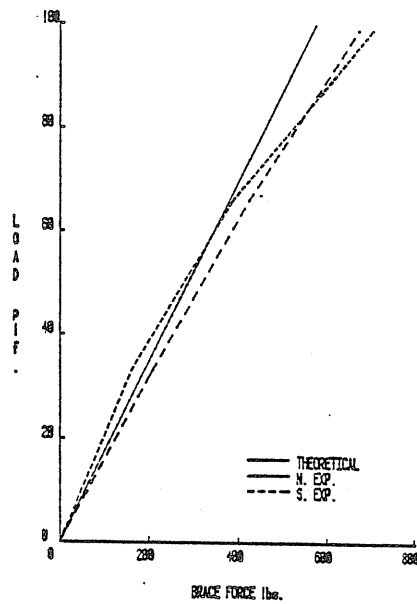
Type	: Full Scale
Span(s)	: 1
Span Length	: 22.3 ft.
Restraint Configuration	: Torsional
Purlin Lines	: 2
Purlin Depth	: 8.0 in.
Material Thickness	: 0.088 in.

b) Test Parameters

Figure B.4 Experimental and Analytical Results for
Test B/2-1-A from Reference [6]

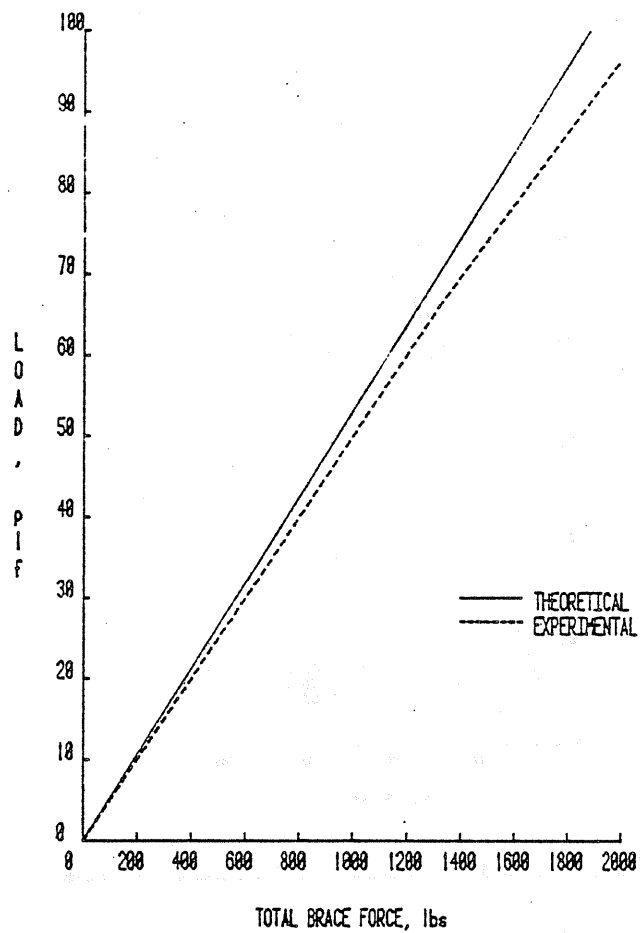


c) Applied Load versus External Brace Forces



d) Applied Load versus Internal Brace Forces

Figure B.3 Experimental and Analytical Results for
Test 3A/2-1, continued

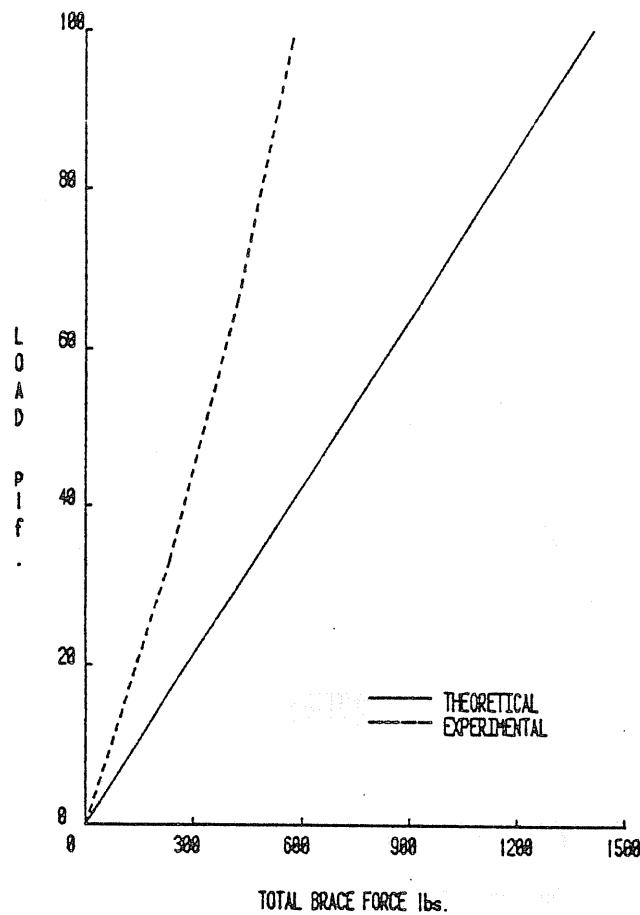


a) Applied Load versus Total Brace Force

Type	: Full Scale
Span(s)	: 3
Span Length	: 20.0 ft.
Restraint Configuration	: Torsional
Purlin Lines	: 2
Purlin Depth	: 8.0 in.
Material Thickness	: 0.091 in.

b) Test Parameters

Figure B.3 Experimental and Analytical Results for
Test 3A/2-1

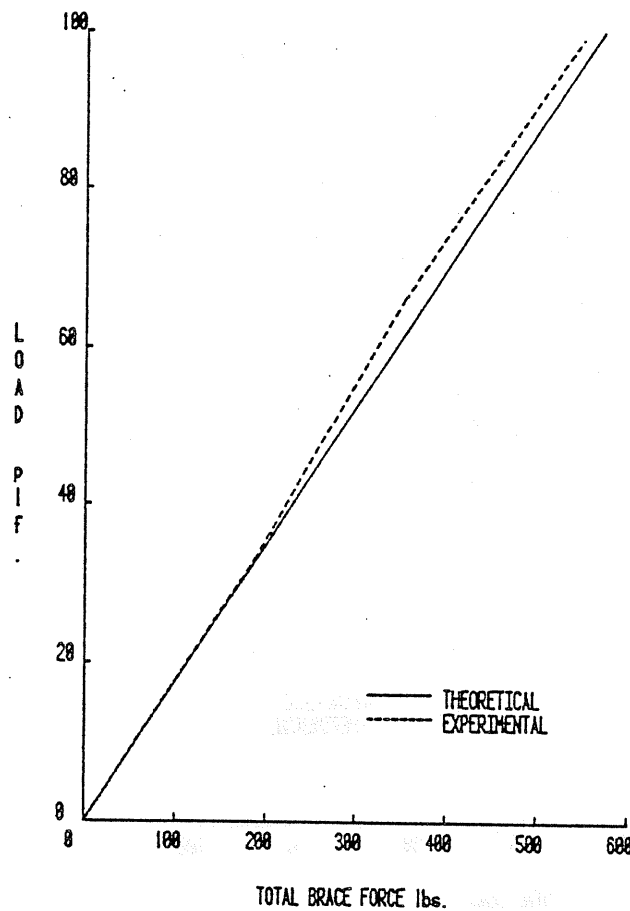


a) Applied Load versus Total Brace Force

Type : Full Scale
Span(s) : 1
Span Length : 14.0 ft.
Restraint Configuration : Torsional
Purlin Lines : 7
Purlin Depth : 8.0 in.
Material Thickness : 0.076 in.

b) Test Parameters

Figure B.2 Experimental and Analytical Results for
Test A/7-2 from Reference [6]



a) Applied Load versus Total Brace Force

Type	: Full Scale
Span(s)	: 1
Span Length	: 14.3 ft.
Restraint Configuration	: Torsional
Purlin Lines	: 2
Purlin Depth	: 8.0 in.
Material Thickness	: 0.074 in.

b) Test Parameters

Figure B.1 Experimental and Analytical Results for
Test A/2-3 from Reference [6]

APPENDIX B

COMPARISON OF ANALYTICAL AND EXPERIMENTAL RESTRAINT FORCES FOR PROTOTYPE TESTS

Applied Load :

On real system :

External purlins : 50 plf

Internal purlin : 100 plf

On stiffness model :

Members 1 to 12 and 25 to 36 :

load in z-direction 1.5556 plf

load in y-direction -3.8654 plf

uniform torque 4.1667 lbs-ft/ft

Members 13 to 24 :

load in z-direction 3.1109 plf

load in y-direction -7.7309 plf

uniform torque 8.3333 lbs-ft/ft

Note : y and z are principal axis (see Figure A.1(a))

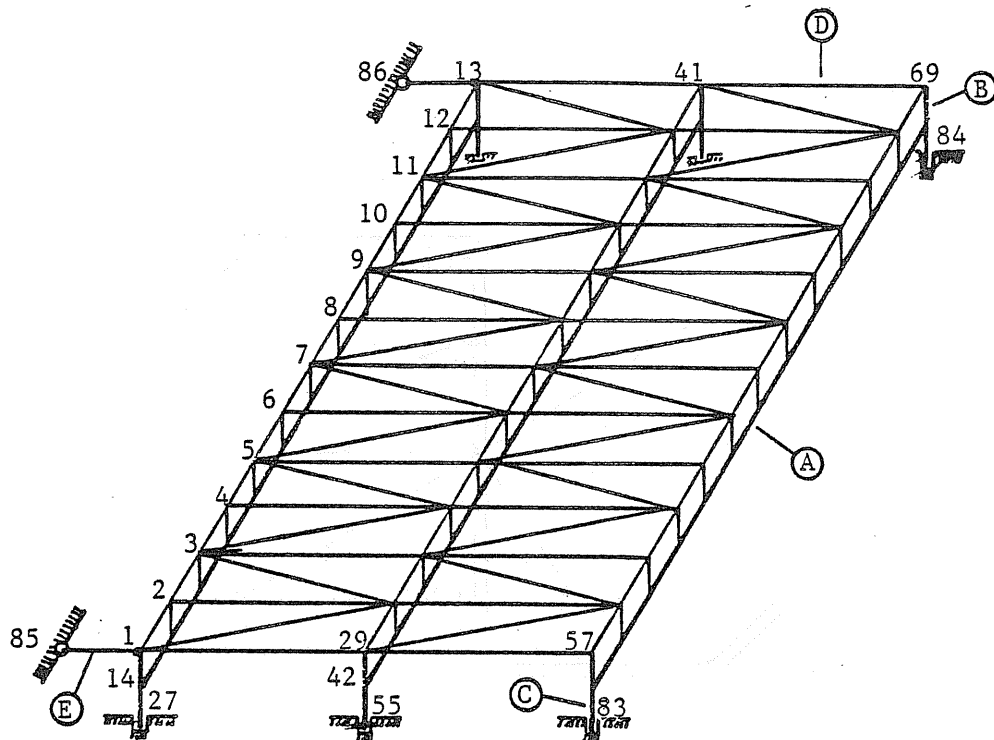
End Conditions :

Members 76 to 81 are free to rotate about the global y-axis at joints 27, 28, 55, 56, 83 and 84, Figure A.2.

Results of Analysis :

A stiffness analysis performed on this model gave the following brace forces

$$B_{f1} = B_{f2} = 487.60 \text{ lbs}$$

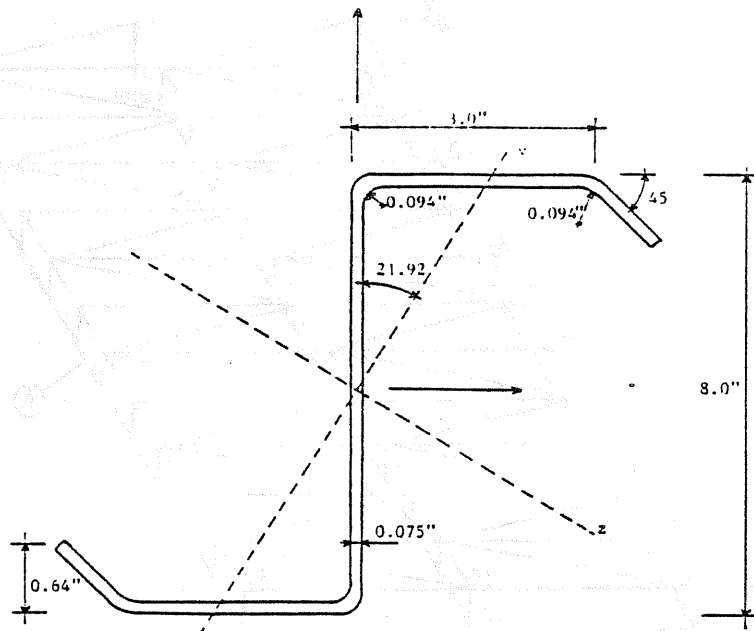


Total Number of Nodes : 86
 Total Number of 12 DOF Elements : 81
 Total Number of 6 DOF Elements : 88
 Total Number of Elements : 169

Member	Area (in ²)	Torsional Constant (in ⁴)	I _y (weak axis) (in ⁴)	I _z (strong axis) (in ⁴)	θ _p (deg.)
A(1)	1.17	10.0	1.11	13.59	21.92
B(2)	1.50	1.11	0.000703	0.0022	0
C(3)	9.00	1.11	0.050625	0.0022	0
D(4)	0.03106	-	-	-	-
E(5)	0.333	-	-	-	-

(1) A : Purlin Members : Elements 1 to 36
 (2) B : Upper Vertical Members : Elements 37 to 75
 (3) C : Lower Vertical Members : Elements 76 to 81
 (4) D : Truss Members : Elements 82 to 16
 (5) E : Bracing Elements : Elements B₁ and B₂

Figure A.2 Joint and Member Numbering and Member Properties



a) Purlin Cross Sectional Geometry

Type	: Torsional restraint
Number of purlin lines	: 3
Number of spans	: 1
Span length	: 20.0 ft.
Purlin spacing	: 5.0 ft.

b) Sample System Parameters

Figure A.1 Cross Section and Parameter Specification

APPENDIX A

SAMPLE INPUT DATA AND RESULTS

10. Freund and Littel, "SAS for Linear Models", SAS Institute, Cary, North Carolina, 1981.
11. SALL, J., "SAS Regression Applications", SAS Institute, Cary, North Carolina, 1981.
12. Cold-Formed Steel Design Manual, American Iron and Steel Institute, Washington, D.C., 1983.

REFERENCES

1. Zetlin, L. and Winter, G. "Unsymmetrical Bending of Beams with and without Lateral Bracing", Proceedings of the American Society of Civil Engineers, Vol. 81, 1955, pp. 774-1 to 774-20.
2. Specification For the Design of Cold-Formed Steel Structural Members, American Iron and Steel Institute, Washington, D.C., September 3, 1980.
3. Needham, J. R., "Review of the Bending Mechanics of Cold-Formed Z-Purlins", Department of Civil Engineering, Univeristy of Kansas, Spring 1981.
4. Ghazanfari, A., and Murray, T. M., "Prediction of Lateral Restraint Forces of Single Span Z-Purlins with Experimental Verification", Fears Structural Engineering Laboratory, Report No. FSEL/MBMA 83-04, University of Oklahoma, Norman, Oklahoma, October, 1983.
5. Ghazanfari, A., and Murray, T. M., "Simple Span Z-Purlin Tests with various Restraint Systems". Fears Structural Engineering Laboratory, Report No. FSEL/MBMA 82-01, University of Oklahoma, Norman, Oklahoma, October, 1983.
6. Curtis, L. E., and Murray, T. M., "Simple Span Z-Purlin Tests to Determine Brace Force Accumulation", Fears Structural Engineering Laboratory, Report No. FSEL/MBMA 83-02, University of Oklahoma, Norman, Oklahoma, July, 1983.
7. Seshappa, V., "Experimental Studies of Z-Purlin Supported Roof Systems Using Quarter Scale Models", A thesis in preparation to be submitted to Univeristy of Oklahoma, Norman, Oklahoma, 1985.
8. Luttrell, D. L., Steel Deck Institute Diaphragm Design Manual, Steel Deck Institute, St. Louis, Missouri, January, 1981.
9. ICES STRUDL-II, The Structural Design Language, IUG Version V3MO, Massachusetts Institute of Technology, Department of Civil Engineering, June 1976.

Equation 5.3 (single span system with torsional restraints) applies with $b_f=3.0$ in., $d=8.0$ in., $t=0.075$ in., $\theta=0$ and n_p is taken as 20:

$$F_b = 0.5 \left[\frac{0.220 (3.0)^{1.500}}{(20)^{0.716} (8.0)^{0.901} (0.075)^{0.600}} - 0 \right] 48000$$

$$= 2333.8 \text{ lbs.}$$

Total brace force is $F_{bt} = 2 (2333.8) = 4667.6$ lbs and the percent brace force is $(4667.6/48000)(100\%)$ or 9.7 %.

Example 7. Same as Example 5 except use one purlin only (load is 100 plf and span is 20 ft).

Solution. Total vertical load to be stabilized

$$W = (20 \text{ ft}) (100 \text{ plf}) = 2000 \text{ lbs}$$

Equation 5.3 (single span system with torsional restraint) applies with $b_f=3.0$ in., $d=8.0$ in., $t=0.075$ in., $\theta=0$ and $n_p = 4$, but Since the number of purlins is less than four, the result must be multiplied by 1.1. Hence

$$F_b = 1.1(0.5) \left[\frac{0.220 (3.0)^{1.500}}{(4)^{0.716} (8.0)^{0.901} (0.075)^{0.600}} - 0 \right] 2000$$

$$= 338.6 \text{ lbs.}$$

Total brace force is $F_{bt} = 2 (338.6) = 677.2$ lbs and the percent brace force is $(677.2/2000)(100\%)$ or 33.9 %.

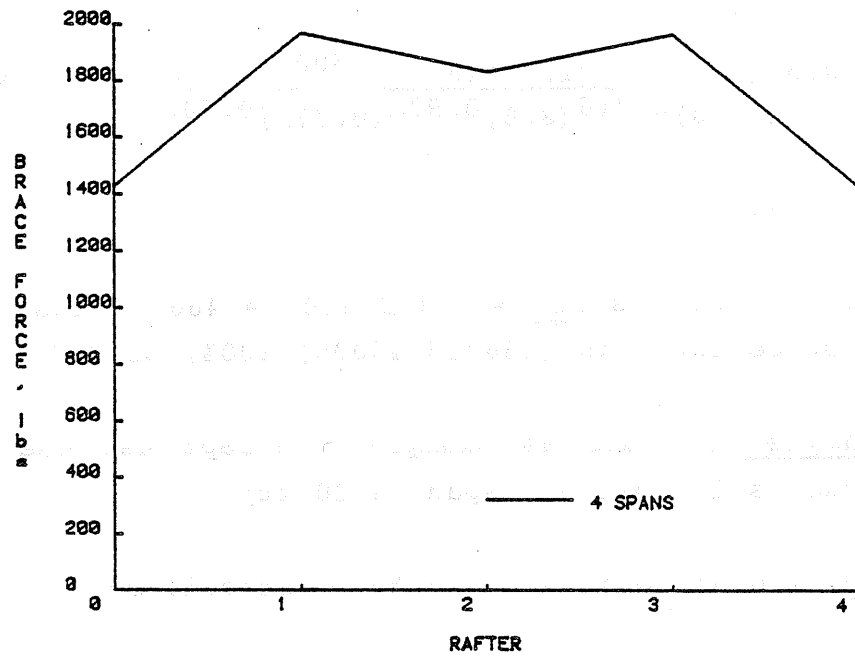


Figure 5.1 Brace Force Distribution for Example 4

Figure 5.1 shows the brace force distribution for this system. The total brace force can be obtained by adding up forces in all braces, that is

$$\begin{aligned} F_{bt} &= 2F_{be} + 2F_{bi1} + F_{bi2} \\ &= 2 (1436.0) + 2 (1983.0) + 1846.3 \\ &= 8684.3 \text{ lbs} \end{aligned}$$

The percent brace force is $[8629.4/(4 (10000))](100\%)$ or 21.7 %

Example 5. Determine brace forces for a single span, two purlin line roof system with torsional braces. Use the purlin cross section shown in Figure A.1, a 20 ft span and a uniformly distributed load of 100 plf.

Solution. The total load to be stabilized is

$$W = 2(20 \text{ ft}) (100 \text{ plf}) = 4000 \text{ lbs}$$

Equation 5.3 (single span system with torsional restraints) applies with $b_f=3.0$ in., $d=8.0$ in., $t=0.075$ in., $\theta = 0$ and $n_p = 4$, but since the number of purlin lines is less than four, the result must be multiplied by 1.1. Hence

$$F_b = 1.1(0.5) \left[\frac{0.220 (3.0)^{1.500}}{(4)^{0.716} (8.0)^{0.901} (0.075)^{0.600}} - 0 \right] 4000$$

$$= 677.2 \text{ lbs.}$$

Total brace force is then $F_{bt} = 2 (677.3) = 1354.6 \text{ lbs}$ and the percent brace force is $(1354.6/4000)(100\%)$ or 33.9 %.

Example 6. Same as Example 5 except use 25 purlins with 50 plf on external purlins and 100 plf on remaining ones.

Solution. Total applied vertical load

$$W = [23(100 \text{ plf}) + 2(50 \text{ plf})] (20 \text{ ft}) = 48000 \text{ lbs.}$$

Total brace force for the sloped roof is $F_{bst} = 1091.3$ lbs and the percent brace force = $(1091.3/8000)(100\%)$ or 13.6 %

Example 4. Determine lateral restraint forces for a four span, five purlin line roof system with torsional braces at the rafters. Use the purlin cross section shown in Figure A.1(a) with 20 ft. span. Load is uniformly distributed and is 25 psf. Purlin spacing is 5 ft. Roof slope is zero.

Solution. The vertical load to be stabilized is (per span)

$$W = 4 (20 \text{ ft}) (5 \text{ ft}) (25 \text{ psf}) = 10000 \text{ lbs}$$

Equation 5.6 (multiple span system with torsional restraint) applies with $b_f = 3.0$ in., $d = 8.0$ in., $t = 0.075$ in., $L = 240$ in. and $n_p = 5$.

i) Braces at the outermost (external) rafters:

$$F_{be} = (0.63) \left[\frac{0.053 (3.0) 1.880 (240) 0.130}{(5) 0.950 (8.0) 1.070 (0.075) 0.940} - 0 \right] 10000$$

$$= 1436.0 \text{ lbs.}$$

ii) Braces located at the first internal rafters:

$$F_{bi1} = (0.87) \left[\frac{0.053 (3.0) 1.880 (240) 0.130}{(5) 0.950 (8.0) 1.070 (0.075) 0.940} - 0 \right] 10000$$

$$= 1983.0 \text{ lbs.}$$

iii) Brace at remaining rafter:

$$F_{bi2} = (0.81) \left[\frac{0.053 (3.0) 1.880 (240) 0.130}{(5) 0.950 (8.0) 1.070 (0.075) 0.940} - 0 \right] 10000$$

$$= 1846.3 \text{ lbs.}$$

b) Roof with 1:12 slope ($\tan \theta = 1/12$)

$$F_{bs} = 0.5 \left[\frac{0.474 (3.0)^{1.521}}{(5)^{0.574} (8.0)^{0.890} (0.075)^{0.325}} - \frac{1}{12} \right] 8000$$

$$= 709.4 \text{ lbs.}$$

Total brace force for the sloped roof is $F_{bst} = 2 (709.4) = 1418.8 \text{ lbs}$ and the percent brace force is $(1418.8/8000)(100\%)$ or 17.7 %

Example 3. Same as Example 1 except use midspan braces.

Solution. The total vertical load to be stabilized is 8000 lbs.

Equation 5.5 (single span system with midspan restraints) applies with $b_f=3.0 \text{ in.}$, $d=8.0 \text{ in.}$, $t=0.075 \text{ in.}$, and $n_p=5$.

a) Zero roof slope ($\tan \theta = 0$)

$$F_b = \left[\frac{0.224 (3.0)^{1.324}}{(5)^{0.648} (8.0)^{0.830} (0.075)^{0.500}} - \tan(\theta) \right] 8000$$

$$= 1758.0 \text{ lbs.}$$

The total brace force is also $F_{bt} = 1758.0 \text{ lbs}$ and the percent brace force is $(1758.0/8000)(100\%)$ or 22.0 %

b) Roof with 1:12 slope ($\tan \theta = 1/12$)

$$F_{bs} = \left[\frac{0.224 (3.0)^{1.324}}{(5)^{0.648} (8.0)^{0.830} (0.075)^{0.500}} - \frac{1}{12} \right] 8000$$

$$= 1091.3 \text{ lbs.}$$

(b) Roof with 1:12 slope ($\tan \theta = 1/12$)

$$F_{bs} = 0.5 \left[\frac{0.220 (3.0) 1.500}{(5) 0.716 (8.0) 0.901 (0.075) 0.600} - \frac{1}{12} \right] 8000$$

$$= 716.2 \text{ lbs.}$$

Total brace force for the sloped roof is then $F_{bst} = 2 (716.2) = 1432.4$ lbs and the percent brace force is $(1432.4/8000)(100\%)$ or 17.9 %

Example 2: Same as Example 1 except use third point braces.

Solution: The total vertical load to be stabilized is 8000 lbs.

Equation 5.4 (single span system with third point restraints) applies with $b_f = 3.0$ in., $d = 8.0$ in., $t = 0.075$ in., and $n_p = 5$.

a) Zero roof slope ($\tan \theta = 0$)

$$F_b = 0.5 \left[\frac{0.474 (3.0) 1.215}{(5) 0.574 (8.0) 0.890 (0.075) 0.325} - 0 \right] 8000$$

$$= 1042.8 \text{ lbs.}$$

Total brace force is then $F_{bt} = 2 (1042.8) = 2085.6$ lbs and the percent brace force is $(2085.6/8000)(100\%)$ or 26.1%

Equations 5.3 to 5.8 using $n_p = 20$. The results will again be conservative.

5.3 Illustrative Examples

Seven examples are given in this Section to illustrate the proposed design procedures. The section shown in Figure A.1(a) will be used for all calculations. This section satisfies the minimum edge stiffener requirements of Section 2.3.2 of the AISI Specification [2]. A span length of 20 ft. is used in all the examples.

Example 1: Determine lateral restraint requirements for a single span, five purlin line roof system with torsional braces at the rafters. Use the purlin cross-section shown in Figure A.1(a) and a load of 100 plf on every internal purlin and 50 plf on the external ones. Consider: (a) a zero roof slope and (b) a 1:12 roof slope.

Solution: The total vertical load to be stabilized is

$$W = [2(50) + 3(100)] \times 20 = 8000 \text{ lbs}$$

Equation 5.3 (single span system with torsional restraint) applies with $b_f = 3.0$ in., $d = 8.0$ in., $t = 0.075$ in. and $n_p = 5$.

(a) Zero roof slope ($\tan \theta = 0$)

$$F_b = 0.5 \left[\frac{0.220 (3.0)^{1.500}}{(5) 0.716 (8.0) 0.901 (0.075) 0.600} - 0 \right] 8000$$

$$= 1049.5 \text{ lbs.}$$

Total brace force is then $F_{bt} = 2 (1049.5) = 2099$ lbs and the percent brace force is $(2099/8000)(100\%)$ or 26.2%

$C_{th} = 0.48$ for all other braces

6. Multiple Span System with Midspan Restraints:

The following provision applies for multiple purlin systems with two or more continuous spans, braced against lateral movement at the center of each span of the braced purlin. The force in each brace depends on its location (external span or internal span) and is given by

$$F_b = C_{ms} \frac{[0.116 (b_f)^{1.320} (L)^{0.180} - \tan(\theta)] W}{(n_p)^{0.701} (d)^{1.000} (t)^{0.500}} \quad (5.8)$$

where $C_{ms} = 1.05$ for braces in the external spans

$C_{ms} = 0.90$ for all other braces.

Brace Forces when $n_p < 4$: Stiffness model analyses performed on different sets of two, three and four purlin line systems showed that the ratio of total brace force to total applied load increased by 5 to 10% when the number of purlin lines is decreased from four to two. Thus, brace forces for a system having less than four purlin lines can be determined from Equations 5.3 to 5.8 by using $n_p = 4$ and multiplying the result by a factor equal to 1.1. It was noted that the results obtained by applying this provision are conservative.

Brace Forces when $n_p > 20$: Variation of the percent brace force was found to be less than 10% when the number of purlin lines is increased over about fifteen. Thus, for design purposes, the percent brace force of a roof system having more than twenty purlin lines can conservatively be taken as the same as for that of a system having twenty purlin lines. That is, brace forces in a system having more than twenty purlin lines can be determined from

3. Single Span System with Midspan Restraint:

The following provision applies for multiple purlin, single span roof systems with one brace attached at the midspan of the braced purlin. The force in the brace is

$$F_b = \left[\frac{0.224 (b_f)^{1.324}}{(n_p)^{0.648} (d)^{0.830} (t)^{0.500}} - \tan(\theta) \right] W \quad (5.5)$$

4. Multiple Span System with Torsional Restraints:

The following provision applies for multiple purlin line systems with two or more continuous spans, braced against lateral movement at every rafter of every span: The force in each individual brace depends on its location (external span, internal span, etc.) and is given by

$$F_b = C_{tr} \left[\frac{0.053 (b_f)^{1.880} (L)^{0.130}}{(n_p)^{0.950} (d)^{1.070} (t)^{0.940}} - \tan(\theta) \right] W \quad (5.6)$$

where $C_{tr} = 0.63$ for the braces at the external rafters
 $C_{tr} = 0.87$ for the braces at the first internal rafters
 $C_{tr} = 0.81$ for braces at remaining rafters

5. Multiple Span System with Third Point Restraints:

The following provision applies for multiple purlin systems with two or more continuous spans, braced against lateral movement at every third point of every span of the braced purlin. The force in each brace depends on its location (external span, internal span, etc.) and is given by

$$F_b = C_{th} \left[\frac{0.181 (b_f)^{1.150} (L)^{0.250}}{(n_p)^{0.536} (d)^{1.110} (t)^{0.289}} - \tan(\theta) \right] W \quad (5.7)$$

where $C_{th} = 0.57$ for outer braces in external spans

satisfy the following:

$$80 \leq (d/t) \leq 110 \quad (5.1)$$

$$25 \leq (b_f/t) \leq 40 \quad (5.2)$$

Edge stiffener dimensions must satisfy the requirements of Section 2.3.2 of the AISI Specifications [2]. The length of a span must not be less than 15 ft., nor greater than 40 ft. The braces are assumed to be connected to only one purlin line in the set. Forces are assumed to be transmitted to the other purlin lines thru the roof deck and its fastening system.

Brace Forces when $4 < n_p < 20$: The following equations (see Chapter IV for development) give the force in each individual brace of a system:

1. Single Span System With Torsional Restraints:

The following provision applies for multiple purlin, single span roof systems having braces at the rafter locations (one brace at each rafter). The force per brace is given by

$$F_b = 0.5 \left[\frac{0.220 (b_f)^{1.500}}{(n_p)^{0.716} (d)^{0.901} (t)^{0.600}} - \tan(\theta) \right] W \quad (5.3)$$

2. Single Span System with Third Point Restraints:

The following provision applies for multiple purlin, single span roof systems with braces attached to the third points of the braced purlin. The force per brace is given by

$$F_b = 0.5 \left[\frac{0.474 (b_f)^{1.215}}{(n_p)^{0.574} (d)^{0.890} (t)^{0.325}} - \tan(\theta) \right] W \quad (5.4)$$

bracing configurations. A parametric study was then carried out and the prediction equations were found to be consistent with the stiffness model. The proposed design procedure is applicable for roof systems with any number of purlin lines and spans, however, limitations on the purlin cross section dimensions exist.

5.2 Proposed Design Procedure

The purpose of the design method is to supply the designer an equation to determine forces in lateral restraint braces which are located at either every rafter, midspan or third point of every span and which are used to stabilize a set of purlin lines under gravity loading. In the following, b_f is the width of the flange as defined in Figure 1.1, d and t are the purlin depth and thickness, and L is the length of a single span. The units for these variables must be "inches". The vertical load applied to all purlin lines in each span of the system is W . The number of purlin lines is designated as n_p , while C is a constant that depends on the bracing configuration and position of the brace. The roof may be inclined any angle θ from the horizontal. Finally, F_b is the force to be calculated for each individual brace.

Variables: Data that pertains to geometry of the system, mainly, purlin cross sectional dimensions, number of spans, number of purlin lines, roof slope, bracing configuration and applied vertical load, constitute the independent variables. The dependent variable is the brace force.

Limitations: Purlin depth-to-thickness ratios (d/t) and flange-width to flange-thickness ratios (b_f/t) must

CHAPTER V

DESIGN PROCEDURE AND EXAMPLES

5.1 General

The goal of this study was to develop a design procedure for lateral restraint requirements for various bracing configurations for Z-purlin supported roof systems with any number of spans and purlin lines. Prior experimental work showed that restraint forces vary considerably with the number of purlin lines and the bracing configuration. However, current design specification provisions to estimate the magnitude of brace forces require only the purlin cross-sectional properties and the vertical load applied to a purlin within a specified distance from the brace location. In most cases, these provisions give very conservative results.

The design procedure given in this Chapter is based on the first order, elastic stiffness model developed in Chapter II. Results of laboratory tests were used to calibrate the stiffness model as explained in Chapter III. The model was used to analyze a set of roof systems with various parameters to determine lateral restraint requirements. Regression analyses were then performed on the collected data and equations to predict lateral restraint forces were presented in Chapter IV for three

4.4 Conclusions

The stiffness model, shown to be adequate to predict real roof system behavior with regard to restraint forces in Chapter III, was used in this Chapter to develop a series of design equations to predict forces in braces in torsional, third point and midspan restraint systems for either single span or multiple continuous span, multiple purlin line roof systems. The developed equations are written in terms of the purlin basic cross sectional dimensions, number of purlin lines, number of spans, span length in the case of multiple span systems and the load applied to the system. These equations were shown to be sufficiently accurate for design purposes when the parameters are kept within the limits specified in Section 4.2. In the next Chapter, these equations will be integrated into a design procedure with roof slope also considered.

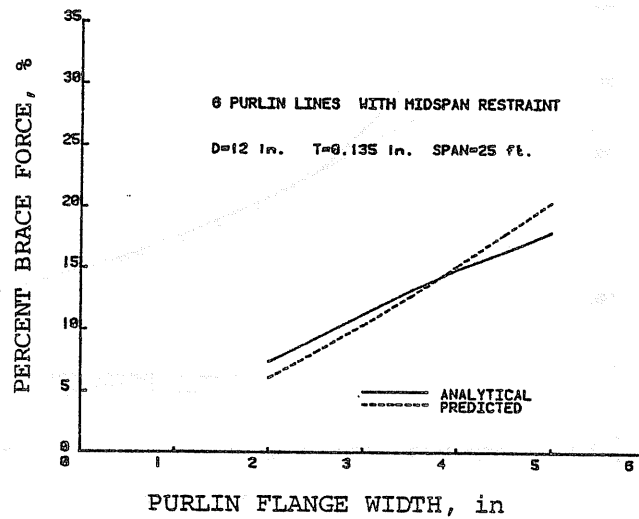


Figure 4.15 Predicted and Theoretical Variation of Percent Brace Force with Purlin Flange Width

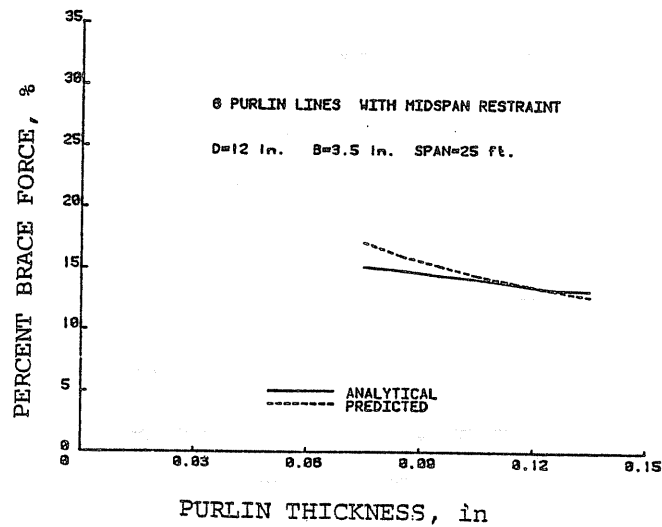


Figure 4.16 Predicted and Theoretical Variation of Percent Brace Force with Purlin Thickness

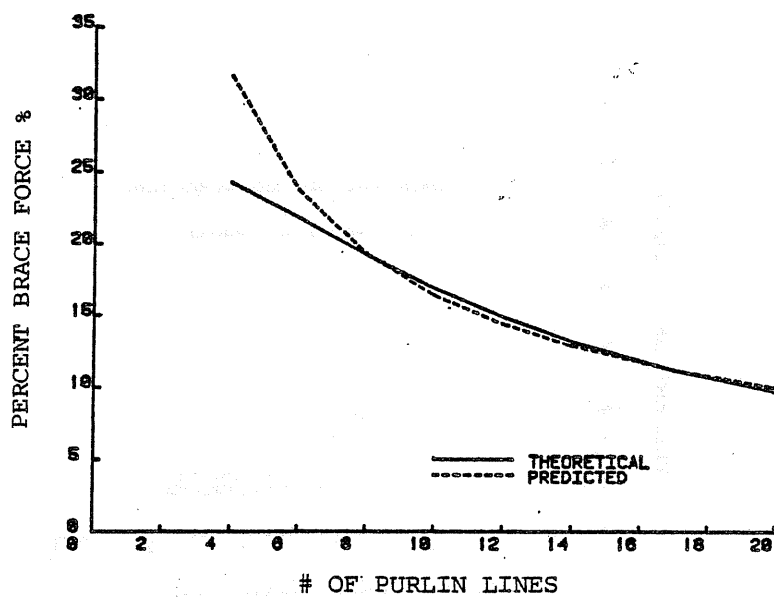


Figure 4.13 Predicted and Theoretical Variation of Percent Brace Force with Number of Purlin Lines

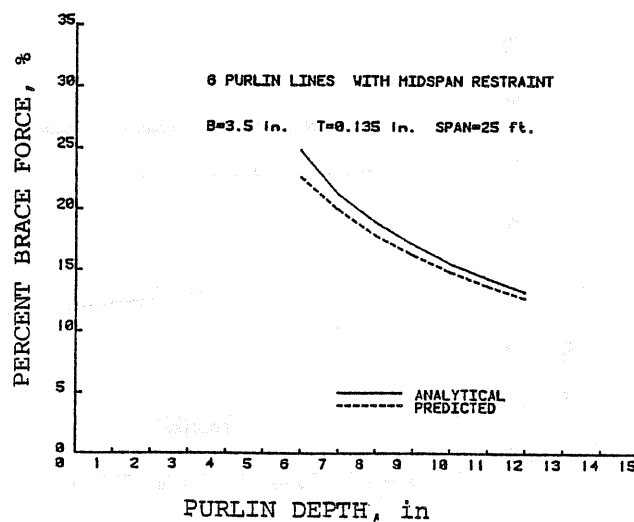
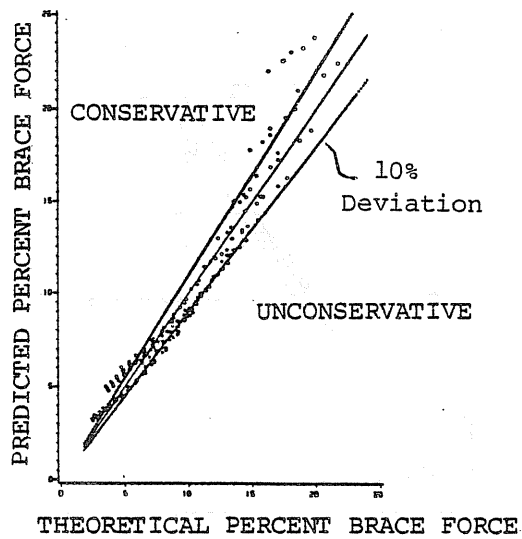
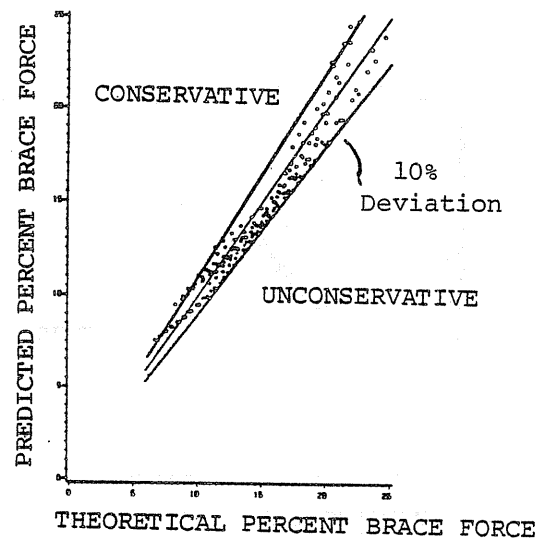


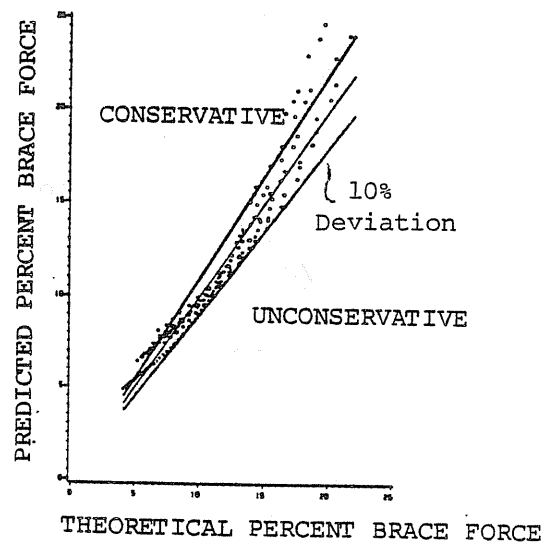
Figure 4.14 Predicted and Theoretical Variation of Percent Brace Force with Purlin Depth



a) Torsional Restraint

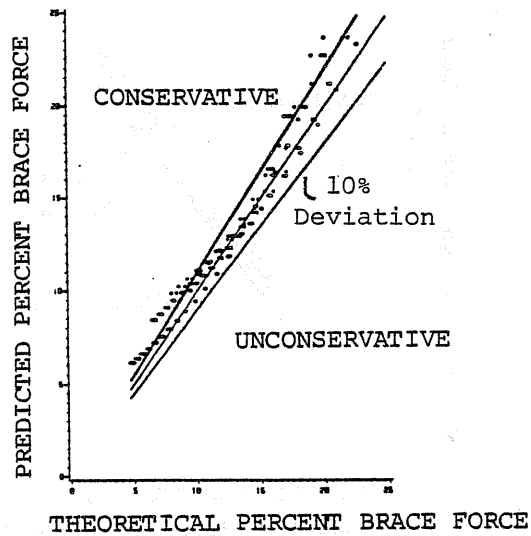


b) Third Point Restraint

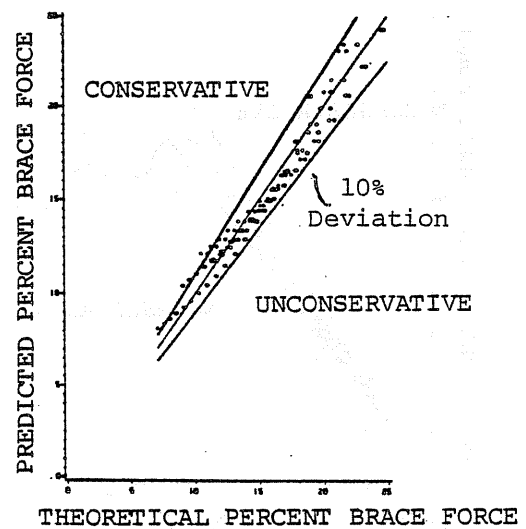


c) Midspan Restraint

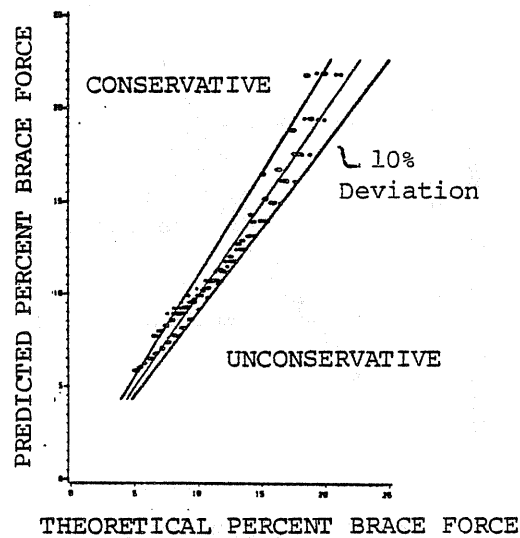
Figure 4.12 Predicted versus Theoretical Percent Brace Force for Three Span Systems



a) Torsional Restraint



b) Third Point Restraint



c) Midspan Restraint

Figure 4.11 Predicted versus Theoretical Percent Brace Force for Single Span Systems

(from the stiffness model), along with the 10% error limit. These graphs are shown in Figures 4.11 and 4.12 for torsional restraint, third point restraint and midspan restraint, for single and three span systems, respectively. By examining these graphs, it was found that the prediction equations for single span systems satisfied the confidence interval criterion better than the three span equations. In the latter case, the 10% significance level criterion was not satisfied in some cases for small number of purlin lines (4 to 6) or for large number of purlin lines (18 to 20). The greatest deviations from the criterion were for large number of purlin lines and were conservative. The absolute error of the predicted brace force did not exceed 2 % except for a few cases.

The final step was to check that the variation of lateral restraint forces due to variations of the purlin dimensions is the same as found when using the stiffness model directly. This was done by performing a parametric study similar to the one discussed in Section 4.3.2, but using the prediction equations instead of the stiffness model, and then comparing the results from both the methods. Lateral restraint forces varied as expected with respect to the number of purlin lines as can be seen in Figure 4.13. Purlin span length did not have a significant effect on percent brace force as was also found when using the stiffness model. The effect of purlin cross sectional properties on lateral restraint was similar to the one predicted by the stiffness model, especially when the flange width to thickness and total depth to thickness ratios are within the limits specified in Section 4.2. Figures 4.14, 4.15 and 4.16 show effect on brace force when purlin depth, flange width and thickness are varied. Both the stiffness model and the prediction equation results are shown.

5. Multiple span system with third point restraints:

$$F_b = C_{th} \frac{0.542 (b_f)^{1.150} (L)^{0.250}}{(n_p)^{0.536} (d)^{1.110} (t)^{0.289}} W \quad (4.13)$$

$$(R^2 = 0.9533)$$

where $C_{th} = 0.19$ for outer braces in external spans
 $C_{th} = 0.16$ for all other braces

6. Multiple span system with midspan restraints:

$$F_b = C_{ms} \frac{0.348 (b_f)^{1.320} (L)^{0.180}}{(n_p)^{0.701} (d)^{1.000} (t)^{0.500}} W \quad (4.14)$$

$$(R^2 = 0.9515)$$

where $C_{ms} = 0.35$ for braces in external spans
 $C_{ms} = 0.30$ for all other braces.

The adequacy of the above equations was first checked by examining the value of the residual R^2 , which is the square of the coefficient of correlation between the real and predicted values of the percent brace force. For the purposes of this study R^2 values greater or equal to 0.9 were considered acceptable (the optimum being 1). The values of R^2 for Equations 4.9 to 4.14 range from 0.94 to 0.96, and are acceptable by this measure.

Further, it was checked to determine if the regression satisfied a "significance level" of 0.10, that is, if the regression error on every value is less than 10% of the true value. For this purpose, the predicted values of the percent brace force were plotted against the true values

distributions in the three span systems. The resulting equations and residual R^2 value are as follows:

1. Single span system with torsional restraints:

$$F_b = 0.5 \frac{0.220 (b_f) 1.500}{(n_p) 0.716 (d) 0.901 (t) 0.600} W \quad (4.9)$$

$$(R^2 = 0.9503)$$

2. Single span system with third point restraints:

$$F_b = 0.5 \frac{0.474 (b_f) 1.215}{(n_p) 0.574 (d) 0.890 (t) 0.325} W \quad (4.10)$$

$$(R^2 = 0.9555)$$

3. Single span system with midspan restraint:

$$F_b = \frac{0.220 (b_f) 1.324}{(n_p) 0.648 (d) 0.830 (t) 0.500} W \quad (4.11)$$

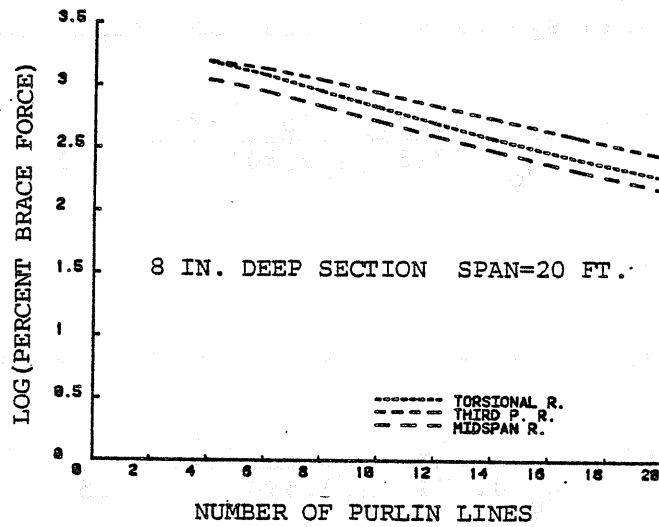
$$(R^2 = 0.9561)$$

4. Multiple span system with torsional restraints:

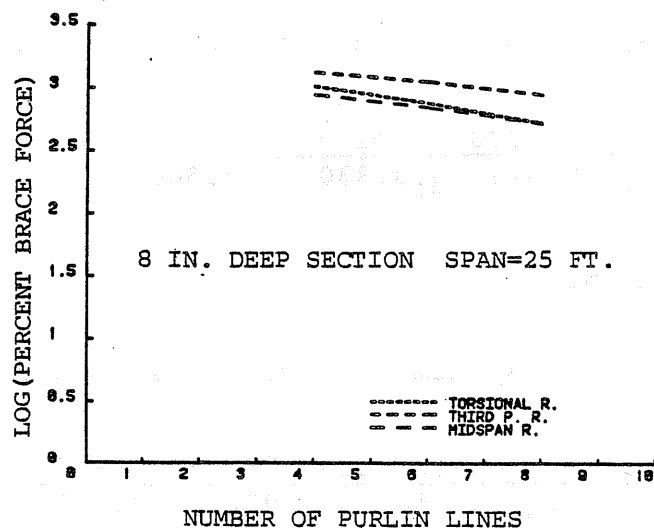
$$F_b = C_{tr} \frac{0.158 (b_f) 1.880 (L) 0.130}{(n_p) 0.950 (d) 1.070 (t) 0.940} W \quad (4.12)$$

$$(R^2 = 0.9401)$$

where $C_{tr} = 0.21$ for braces at external rafters
 $C_{tr} = 0.29$ for braces at first internal rafters
 $C_{tr} = 0.27$ for braces at all other rafters



a) Single Span Systems



b) Three Span Systems

Figure 4.10 Natural Logarithm of Percent Brace Force versus Number of Purlin Lines

A total of 187 data points were generated for each bracing configuration for the single span systems (561 cases). Only 60 data points for each brace configuration were generated for the three span systems because of computer storage and cost limitations. To generate additional data points for the latter systems, the available single and three span results were plotted as shown in Figure 4.10 (natural logarithm of percent brace force versus number of purlin lines). It was observed that both sets of data plot as straight lines. To obtain additional data points for the three span systems, equations were written (assuming linear behavior with respect to the coordinates of Figure 4.10) for each of the three curves shown in Figure 4.10(b). Brace force values were then calculated using these equations for 4 to 20 purlin line roof systems; a total of 204 sample points per brace configuration was generated in this manner.

The dependent variable for all analyses was the percent brace force for the system and the independent variables were b_f , the purlin flange width as defined in Figure 1.1; d , the total depth; t , the material thickness; L , the span length; and n_p , the number of purlin lines. The dimensions used were inches for lengths and pounds for force.

After the equations were developed, they were modified so force acting at each individual brace can be calculated. This force is referred to as F_b . The modifications involved the introduction of W , the total vertical load applied on all purlin lines in each span of the system; and C , a distribution coefficient which depends on the location of the brace (external, internal, etc.). The coefficient C was determined from statistical examination of brace force

TABLE 4.4

Roof Systems Analyzed to Obtain
Data for Regression Analyses Input

(a) Analyses Conducted for Single Span Systems
for Each Brace Configuration

Section	Number of Purlin Lines	Span Lengths (ft)	Total Number Of Systems
S1	4-20	15 20	34
S2	4-20	15 20 25	51
S3	4-20	20 25 30	51
S4	4-20	25 30 35	51
Total number of systems per bracing configuration			187

(b) Analyses Conducted for Three Span Systems
for Each Brace Configuration

Section	Number of Purlin Lines	Span Lengths (ft)	Total Number of Systems
S1	4-8	15 20 25	15
S2	4-8	20 25 30	15
S3	4-8	25 30 35	15
S4	4-8	30 35 40	15
Total number of systems per bracing configuration			60

to the system.

For multiple purlin systems, the position of the braced purlin with respect to the other purlins was found to affect lateral restraint forces. These forces are maximum if the farthest purlin from the ridge or eave is braced and minimum if the ridgemost purlin is braced. The difference can be as large as 6% absolute. If the second purlin is braced, considering the eave purlin as first, the resulting brace forces are very close to the maximum. The difference is approximately 1% absolute.

In the following development of design equations, the location of all braces is assumed to be between the eave and the next "uphill" purlin with the brace connected to the latter purlin.

4.3.3 Regression Analysis

Six equations to predict lateral restraint forces for Z-purlin supported roof systems are developed in this subsection. The first three equations are for single span, multiple purlin line systems, with torsional restraint, third point restraint or midspan restraint. The second three equations apply to multiple span, multiple purlin line systems with torsional restraint, third point restraint or midspan restraint in each span. Each of the six cases is considered individually. Table 4.4 shows the cross-section type (see Subsection 4.3.1) and the span lengths used with each type. Each combination was analyzed and the data was then regressed to obtain the prediction equations.

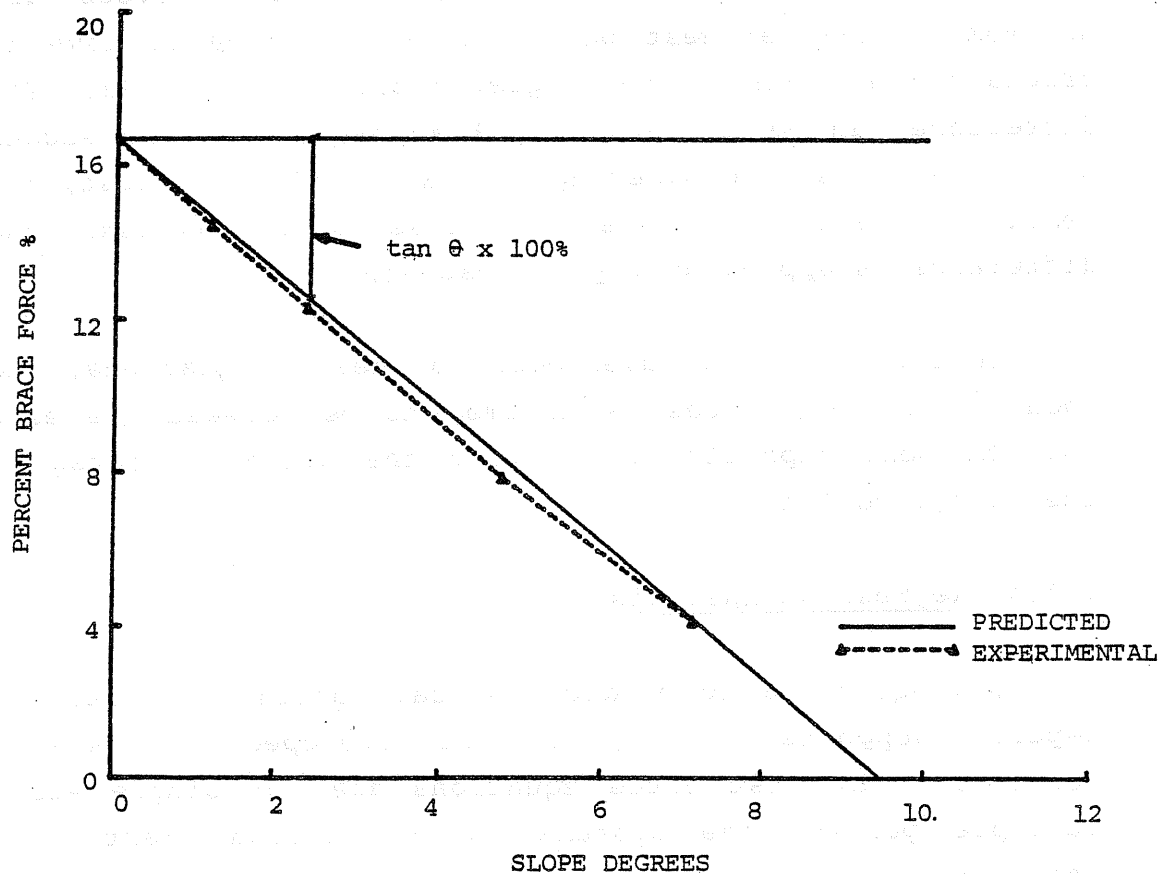
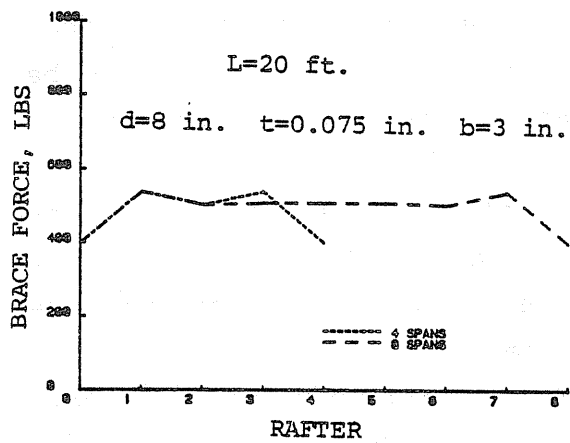
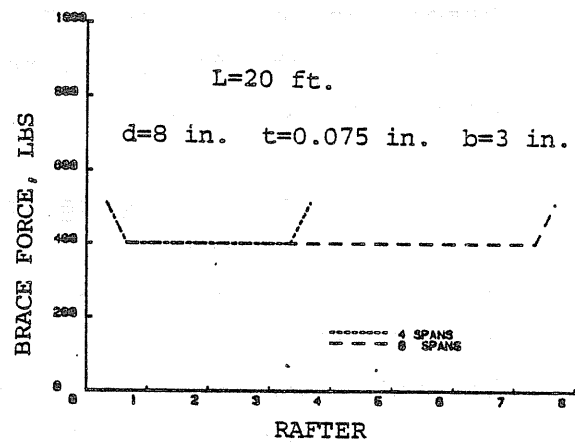


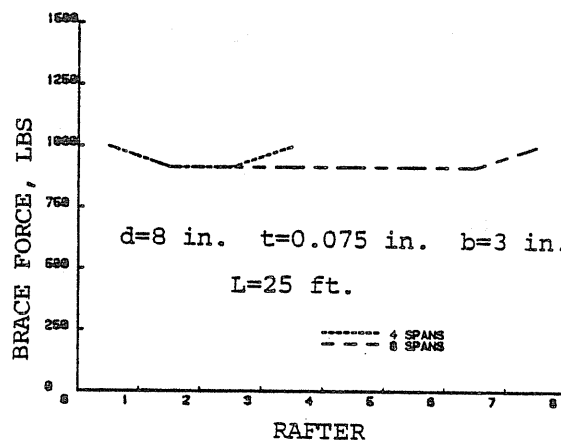
Figure 4.9 Variation of Percent Brace Force with Roof Slope



a) Torsional Restraint



b) Third Point Restraint



c) Midspan Restraint

Figure 4.8 Brace Force Distributions for Multiple Span Systems

made. Figure 4.8 shows typical results. It is clear from the figure that the magnitude of force at a specific location, e.g., exterior, first interior, etc., is the same for four and eight span systems using any of the three brace configurations. Thus, if the total restraint force is known, the force acting on each individual brace can be determined accurately regardless of the number of spans.

Bracing Configuration: Lateral restraint forces cannot be mathematically related to the bracing configuration used, therefore, each configuration must be considered separately. In general, it was found that lateral forces in a third-point restraint system were higher in magnitude than those in a torsional restraint system. Forces in midspan restraint systems were usually slightly lower in magnitude to those found in torsional restraint systems.

Other Effects: An important effect not investigated in the parametric study is roof slope. To experimentally study the effect of roof slope on lateral restraint, Seshappa [7] conducted quarter scale model tests. Slopes of 0:12, 1/4:12, 1/2:12, 1:12 and 1-1/2:12 were considered. He found that lateral restraint forces decrease as a linear function of the roof slope as shown in Figure 4.9. Thus, brace force predictions for zero slope roof can easily be corrected using

$$BF_s = BF_o - W \tan \theta \quad (4.8)$$

where BF_s = total brace force for the sloped roof system, BF_o = total brace force for an identical roof system with zero slope, θ = angle of inclination from the horizontal of the sloped roof system, and W = total vertical load applied

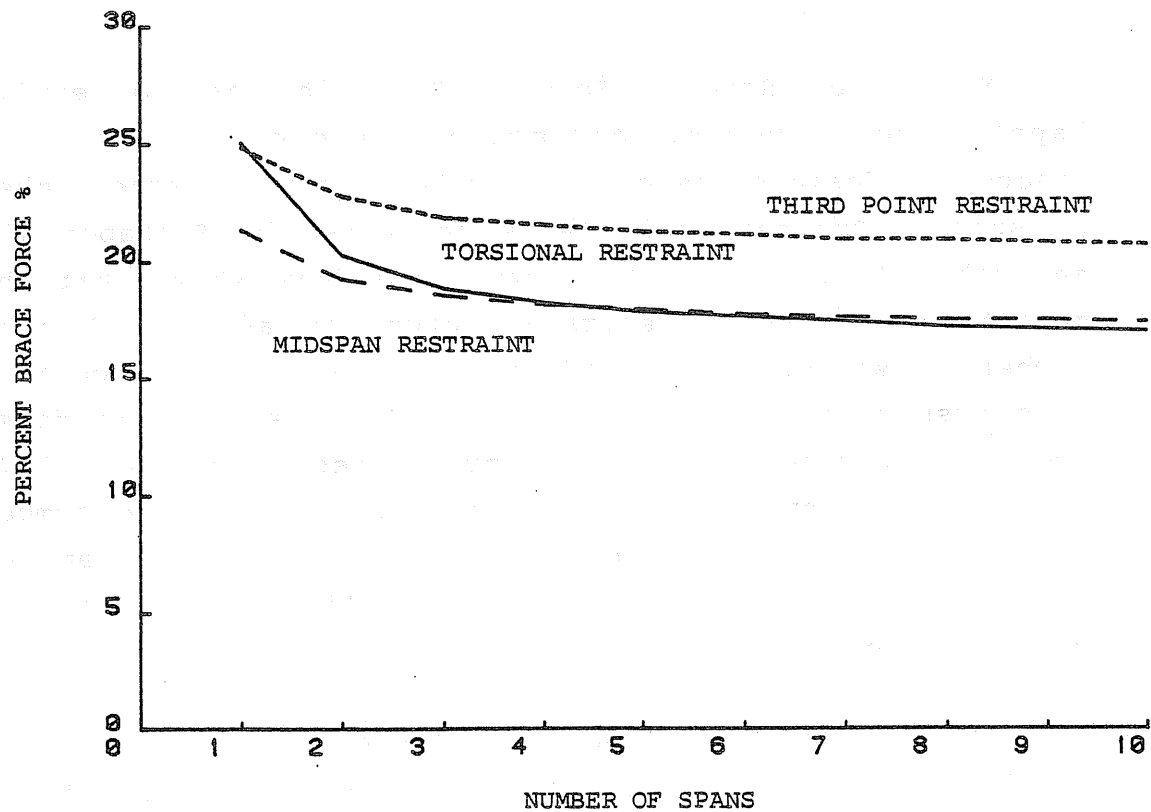


Figure 4.7 Variation of Percent Brace Force with Number of Spans

2. Increasing purlin flange width causes an increase in lateral restraint forces.
3. Lateral restraint forces decrease slightly when purlin thickness is increased.

Number of Spans: Because Z-purlins can be easily lapped and a moment connection developed, they are frequently designed as continuous beams over a large number of spans. Quarter scale tests conducted by Seshappa [7] and other full scale laboratory tests have shown that the magnitude of lateral restraint forces is affected by the number of spans. The stiffness model was used to confirm this assumption. A two-purlin line roof system stiffness model was studied with purlin properties of section S2 (8 in. deep section) and a span length of 20 ft. The number of spans was varied between 1 and 10 with an increment of 1. Analyses were performed for the three bracing configurations.

The results are shown in Figure 4.7 as a plot of percent brace force versus the number of spans. As shown, lateral restraint forces decrease significantly (12 to 30%) when the number of spans increases from 1 to 3. A further increase in number of spans does not significantly affect the percent brace force. For example, the difference between the percent brace force of a three-span system and that for a ten-span system is less than 2% absolute. It follows that the percent brace force of a three-span roof system can be conservatively used for continuous systems having three or more spans.

A further analysis of a variety of multiple span systems to determine the effect of number of spans on the magnitude of restraint force at specific locations was

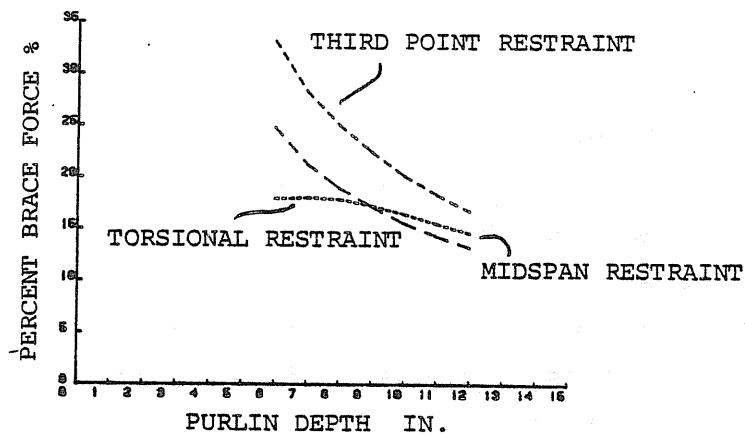


Figure 4.4 Variation of Percent Brace Force with Purlin Depth

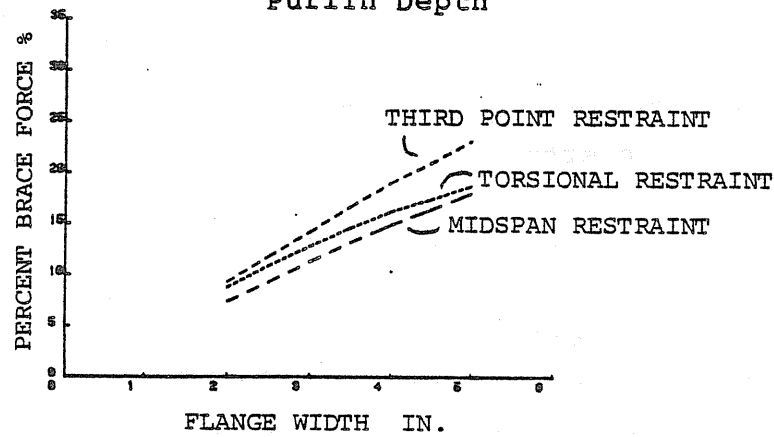


Figure 4.5 Variation of Percent Brace Force with Purlin Flange Width

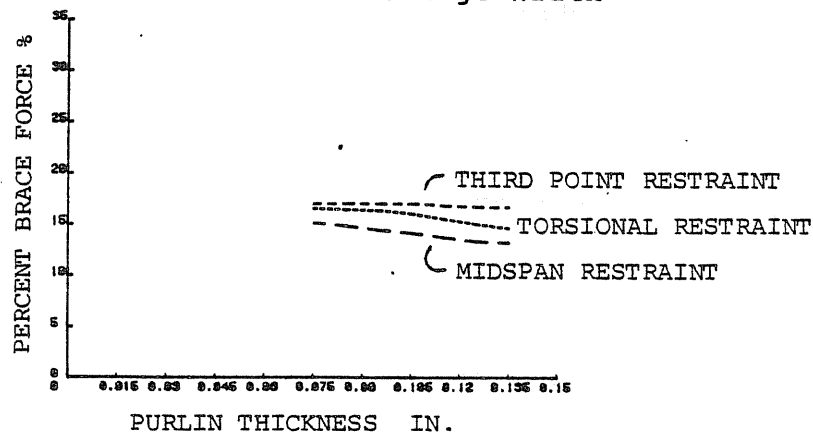


Figure 4.6 Variation of Percent Brace Force with Purlin Thickness

significantly different.

The second set of systems were used to study the variation of lateral restraint forces with purlin flange width. For this case, both the purlin depth and thickness were kept constant, respectively equal to 12 in. and 0.135 in. Purlin flange width was varied between 2 in. and 5 in. in 0.5 in. increments. Lateral restraint forces were found to increase in a similar way for all three bracing configurations and increasing with increasing flange width, (see Figure 4.5). This behavior can be explained by the fact that the load is applied to the purlin within an eccentricity equal to one third of the flange width from the plane of the web. Increasing this width results in an increase in the overturning torque acting on the purlin.

In the final set, the thickness was varied between 0.075 in. and 0.135 in., in 0.005 in. increments. Purlin depth and flange width were kept constant, respectively equal to 12 in. and 3.5 in. Figure 4.6 illustrates the variation of lateral restraint forces with purlin thickness for the three bracing configurations. It was found that increasing the thickness results in a slight decrease in the percent brace force.

The conclusions drawn from this phase of the parametric study are summarized as follows:

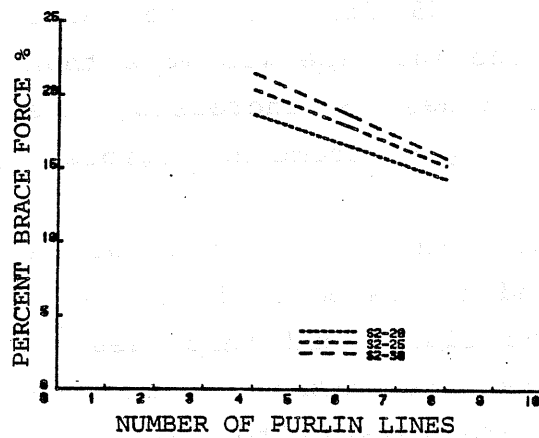
1. Increasing purlin depth results in a decrease of lateral restraint requirements. Forces associated with torsional restraint systems are affected differently than those for third-point or midspan restraint systems.

For the single span, four purlin line systems, it was found that restraint forces increased less than 5% when the span was increased from 15 ft. to 25 ft. For the three span, four purlin line systems, the increase was more than 10%. As the number of purlin lines is increased, the differences associated with span length become negligible.

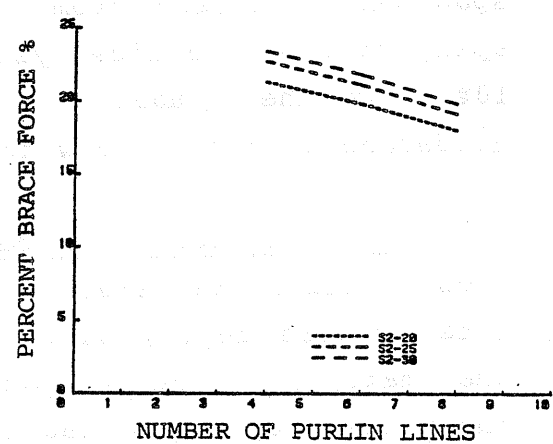
Cross-Sectional Properties: The properties of a cross-section are directly related to its basic dimensions: total purlin depth, width of the flange and thickness of the material. Other parameters are either relatively insignificant, e.g., radii, or are related to the basic dimensions as in the case of the length of the edge stiffener.

To determine the effect of the basic purlin cross-sectional dimensions on the magnitude of lateral restraint requirements for the system, a parametric analysis was carried out using the stiffness model. Three sets of seven single span systems were developed. The span length was fixed at 25 ft. and the number of purlin lines at 6. In the first set, the purlin depth was varied between 6 in. and 12 in., with an increment of 1 in., while the flange width and the thickness were kept constant and equal to 3.5 in. and 0.135 in., respectively. All three bracing configurations were considered. The stiffness model was used for analyses.

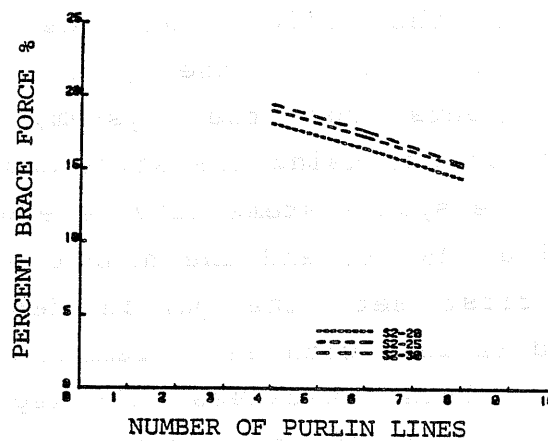
Selected results for this first set are shown in Figure 4.4. From the plot, it is evident that lateral restraint forces vary inversely with purlin depth. Forces associated with midspan restraint and third-point restraint system varied with purlin depth in a similar manner, whereas, the variation for torsional restraint systems was



Torsional Restraint



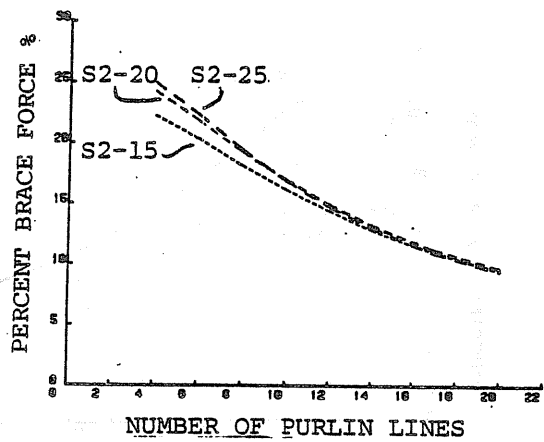
Third Point Restraint



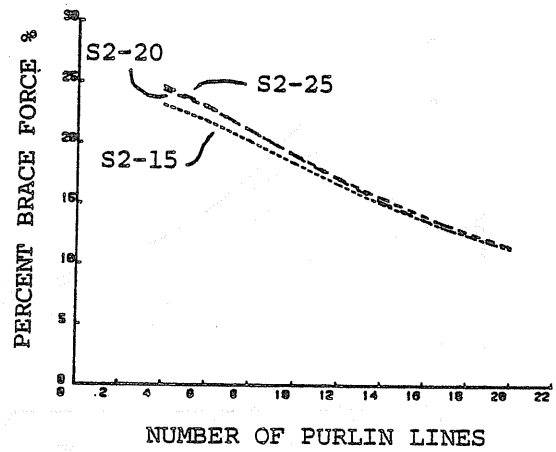
Midspan Restraint

b) Three Span Systems

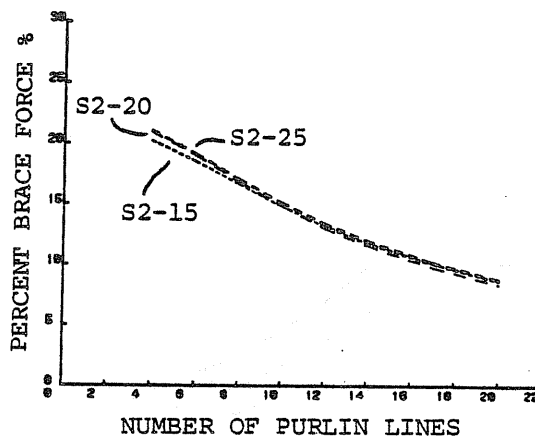
Figure 4.3 Variation of Percent Brace Force with Span Length, continued



Torsional Restraint



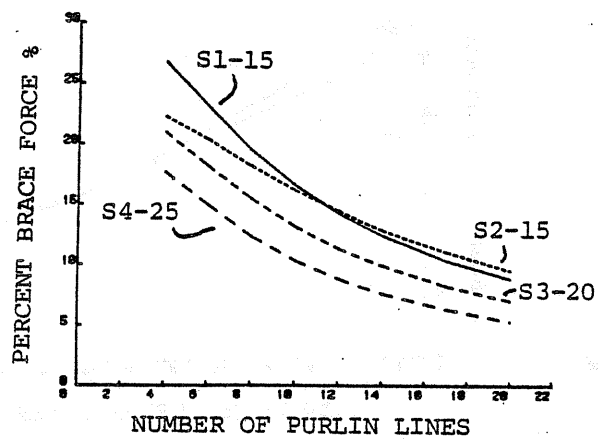
Third Point Restraint



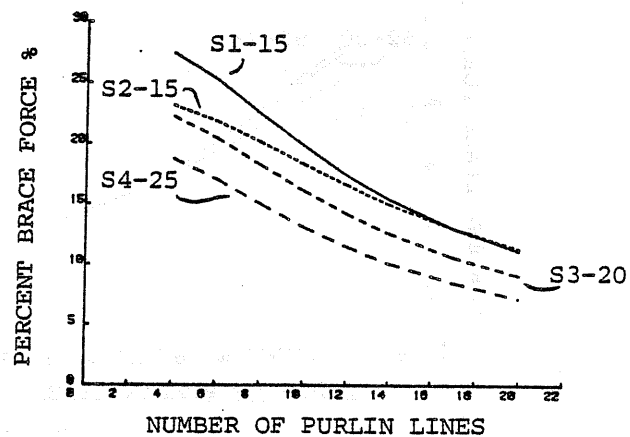
Midspan Restraint

a) Single Span Systems

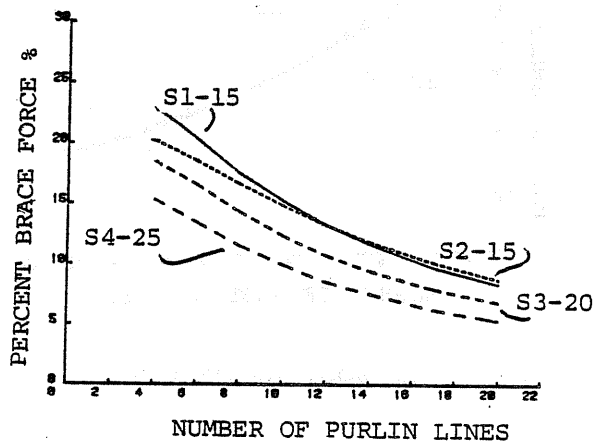
Figure 4.3 Variation of Percent Brace Force with Span Length



a) Torsional Restraint



b) Third Point Restraint



c) Midspan Restraint

Figure 4.2 Variation of Percent Brace Force with Number of Purlin Lines

variation of parameters on system behavior was conducted. The study included the variation of lateral restraint with the following: (1) number of purlin lines, (2) span length, (3) purlin cross-sectional properties, (4) number of spans, and (5) bracing configuration. The results are discussed in the following paragraphs.

Number of Purlin Lines: Prior experimental test results showed that the ratio of lateral restraint forces to the total applied vertical load (the percent brace force) decreases when the number of purlin lines is increased [6,7]. Preliminary analytical analyses of several stiffness models showed that when the number of purlin lines is increased from 4 to 20, the percent brace force may decrease by 55 to 70% relative for torsional and midspan restraints, and by 50 to 60% relative for third point restraint.

More complete results are shown in Figure 4.2. The plots are of percent brace force versus the number of purlin lines for the three bracing configurations, single span systems. The number after the letter S refers to the section as defined in Table 4.1 and the number after the dash refers to the length of the single span. For example S1-15 represents section S1 analyzed at a simple span of 15 ft. It is apparent from Figure 4.2 that the preliminary results are indicative of general results.

Purlin Span Length: The variation of lateral restraint forces with span length is shown in Figure 4.3. Section S2 and spans of 15 ft., 20 ft. and 25 ft. were chosen for the analysis. The number of purlin lines and restraint configuration were varied and both single and three span systems were considered.

TABLE 4.2

Flexural Capacities of Purlin Sections Used
in the Parametric Study
(kip-ft)

Section	Allowable Capacity ¹	Ultimate Capacity ²
S1	4.7	7.9
S2	7.2	12.0
S3	16.4	27.3
S4	28.0	46.8

¹ AISI Specifications [2]

² $M_u = 1.67 M_a$

TABLE 4.3

Ultimate Simple Span Uniformly Distributed Loads
(plf)

Section Name	Span Length (ft)				
	15	20	25	30	35
S1	280.9	158.0	101.1	70.2	51.6
S2	426.7	240.0	153.6	106.7	78.4
S3	970.7	546.0	349.4	242.7	178.3
S4	1664.0	936.0	599.0	416.0	305.6

Equation 4.6 can then be solved for b and assuming the thickness t of the lip is much smaller than b , the minimum vertical lip dimension L_d can be approximated by

$$L_d = b \cos(45^\circ) = b/\sqrt{2} \quad (4.7)$$

The minimum vertical lip dimensions for the four base cross-sections described in Table 4.1 are then 0.60 in., 0.64 in., 0.85 in. and 1.00 in. for Sections S1, S2, S3 and S4, respectively. These dimensions also satisfy the requirement that I_{x1} be greater than $9.2t^4$.

The allowable flexural capacity of each one of the sections was calculated using local buckling criteria from the AISI Specification [2] and assuming cross-sectional stresses distributed as if bending was constrained in the vertical plane, i.e., the flexure formula $f = M y/I$ was assumed to apply. To obtain the ultimate flexural capacity, the allowable capacity was multiplied by the AISI basic factor of safety, 1.67. Results are summarized in Table 4.2. It is noted that the flanges of all four sections were found to be fully effective.

The ultimate flexural capacity is also given in Table 4.3 in terms of uniformly applied vertical load per unit length of purlin for five span lengths per section. These span lengths were used in the parametric study for single span analyses. The lengths were increased 5 ft. each for the multiple span systems.

4.3.2 System Behavior Analysis

Prior to the development of the lateral restraint prediction equations, a study of the effects of the

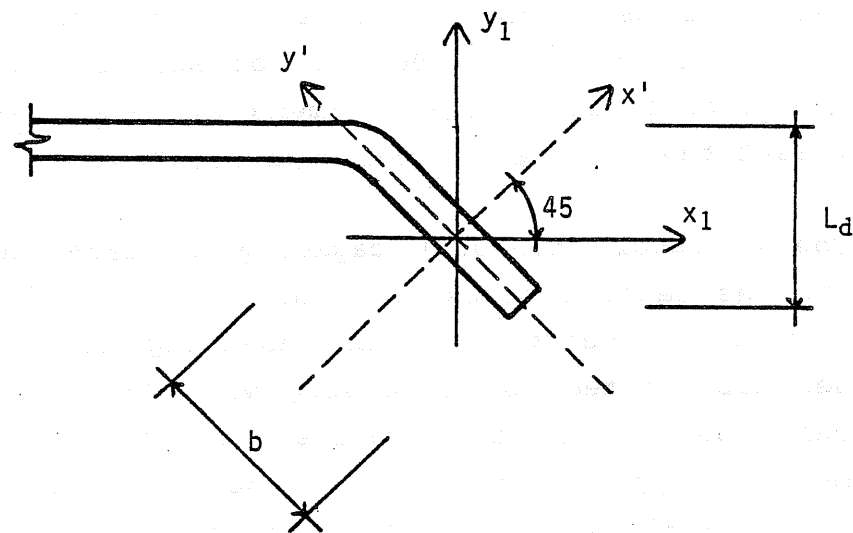


Figure 4.1 Purlin Lip Detail

I_{min} , of an edge stiffener of any shape about its own centroidal axis parallel to the stiffened element shall be greater than the maximum of

$$I_{min} = 1.83 t^4 \sqrt{(w/t)^2 - 4000/F_y} \quad (4.1)$$

and $9.2t^4$, where w and t are respectively the flat width and the thickness in inches of the stiffened element and F_y is the minimum yield strength of the material in ksi.

Referring to Figure 4.1, the moments of inertia of the lip about the x' -axis and y' -axis are, respectively,

$$I_{x'} = tb^3/12 \quad (4.2)$$

and

$$I_{y'} = bt^3/12 \quad (4.3)$$

The moment of inertia of the lip about the x_1 axis, which is parallel to the flange, can be calculated from

$$I_{x1} = (I_{x'} + I_{y'})/2 = (tb^3 + bt^3)/24 \quad (4.4)$$

According to Section 2.3.2 of the AISI Specification [2], I_{x1} should be at least equal to the value of I_{min} given by Equation 4.1, or

$$I_{x1} - I_{min} \geq 0 \quad (4.5)$$

substituting I_{x1} , yields

$$(t/24) b^3 + (b/24) t^3 - I_{min} \geq 0 \quad (4.6)$$

TABLE 4.1
Purlin Cross Sectional Dimensions and Properties
Used in the Parametric Study

Section	S1	S2	S3	S4
d in	6	8	10	12
b _f in	2.5	3	3.5	3.5
t in	0.075	0.075	0.105	0.135
L _d in	0.6	0.64	0.85	1.0
r ₁ in	0.094	0.094	0.188	0.188
r ₂ in	0.094	0.094	0.188	0.188
A in ²	0.935	1.168	2.0	2.89
J in ⁴	0.0018	0.0022	0.0074	0.0177
I _x in ⁴	5.42	11.85	31.22	62.36
I _y in ⁴	1.78	2.85	7.01	10.05
I _{xy} in ⁴	2.34	4.32	10.96	18.19
I _{xy} /I _x	0.432	0.365	0.351	0.292
I _{x'} in ⁴	6.55	13.588	35.44	68.06
I _{y'} in ⁴	0.587	1.112	2.786	4.35
θ _p deg.	25.84	21.92	21.08	17.41

is four to twenty, however, approximations will be offered for systems with less than four and more than twenty purlin lines.

Only commonly used Z-shaped cold-formed purlins (depth to web-thickness ratios of 80 to 110 and flange-width to flange-thickness ratios of 25 to 40) were considered. Edge stiffener dimensions were selected to satisfy the requirements of Section 2.3.2 of the AISI Specification [2]. For this study, the yield stress of the purlin material was arbitrarily taken as 55 ksi. Span lengths were limited from 15 ft. to 40 ft.

Three lateral restraint configurations were considered for both single span and multiple span systems. These configurations were defined in Chapter II as: (1) torsional restraint at the rafters (see Figure 2.1); (2) third point restraints in each span (see Figure 2.2), and (3) midspan restraint in each span (see Figure 2.3).

4.3 Development of the Design Equations

4.3.1 Cross Sections Used

Table 4.1 lists the dimensions and cross sectional properties of four sections (designated as S1, S2, S3 and S4) that were chosen for use in the development of lateral restraint prediction equations. The depth, thickness and flange width of each one of these sections were selected from the AISI Manual Design Tables [12]. The vertical dimension of the stiffening lip was determined so that Section 2.3.2 of the AISI Specification [2], which pertains to edge stiffeners for compression elements, was satisfied. This section requires that the minimum moment of inertia,

CHAPTER IV

DEVELOPMENT OF THE DESIGN PROCEDURE

4.1 Methodology

The stiffness model developed earlier in this study is not a practical design tool, but can be used to develop a simplified design procedure. This can be done by first selecting a variety of purlin cross sectional dimensions and other parameters, such as the number of purlin lines, number of spans and the span length within a chosen practical range, and then determine brace forces corresponding to each set of parameters using the stiffness model. After collecting sufficient data, a statistical regression analysis can be performed to yield a single expression written in terms of the previously defined parameters for the brace force. It is noted that such an expression can be erroneous and unrelated to the actual behavior of the system since it is based only on statistical considerations. Thus, it is necessary to first perform a parametrical study in order to judge the adequacy of the developed equations.

4.2 Limits of Parameters and Configurations

The equations that are to be developed in this study will apply to single or multiple span and multiple purlin line roof systems. The number of purlin lines considered

3.2 Conclusions

First, it is important to note that the quarter scale model tests conducted for this study and those conducted by Seshappa [7] behave exactly in the same way as prototype tests if the effects of restraint prestress forces at low loads are disregarded. This means that the experimental results obtained by conducting such tests reflect what actually happens in real systems.

Good correlations between analytical predictions from the stiffness model developed in Chapter II and experimental results were obtained for both full scale and quarter scale test results. This leads to the conclusion that the proposed stiffness model provides an adequate representation of thru fastener, corrugated steel panel deck, Z-purlin supported roof system behavior. However, use of the stiffness model requires the availability of a computer with large storage capacity and a stiffness program capable of handling twelve degree-of-freedom space frame type elements, and thus is not a practical design tool. In the next chapter, a set of prediction equations for lateral restraint requirements, depending on the bracing configuration, number of spans, number of purlin lines and purlin properties are developed. This was accomplished by first establishing a set of system parameters with practical limitations and then performing regression analyses on sets of data obtained from system analyses using the stiffness model.

The last four tests form the S-series and were conducted expressly for this study. The configuration for all tests was two purlin lines, single span with torsional restraint. Test S1/2-15 used two 1.5 in. deep purlins and 3.75 ft. span, which is the quarter scale model of a prototype test with 6 in. deep purlins and 15 ft. span. Figure C.10 shows the analytical and experimental brace forces with applied load for this test. The correlation is considered very good when the pretensioning effects are considered.

Test S1/2-25 also was conducted with 1.5 in. purlin but the span was 6.25 ft. The configuration corresponds to a prototype test with 6 in. deep purlins and 25 ft. span. The results for this test are shown in Figure C.11. The correlation between analytical and experimental results are good at loads higher than 6 plf, again neglecting prestressing effect.

Figures C.12 and C.13 show the results of the last two tests of the series. Test S4/2-15 used two 3 in. deep purlins with 3.75 ft. span which corresponds to a prototype test with 12 in. deep purlins and 15 ft. span. Test S4/2-25 used the same size purlins with a span of 6.25 ft., corresponding to a prototype span of 25 ft. Correlation between the analytical and experimental results is also good for both of these tests when pretension effects are accounted for. However, from Figures C.12 and C.13 it is apparent that the brace pretensions were not overcome until the load reached approximately 25 plf for test S4/2-15 and 20 plf for test S4/2-25, this is most likely due to an overtightening of the braces before testing.

the correlation between analytical and experimental results for this test is good.

Figure C.2 shows the variation of analytical and experimental brace forces with uniform applied load for a six purlin line, single span test with torsional restraint. Agreement between analytical and experimental results is again good when the pretensioning effects are considered.

Shown in Figure C.3 are the test results of a two purlin line, single span system with third point restraint braces. Agreement between analytical and experimental results is good for this test. This agreement is also good for the test results of a two purlin line, single span system with midspan brace as shown in Figure C.4.

Figures C.5 and C.6 show results for six purlin line, single span tests with third point restraint and midspan restraint, respectively. Agreement between the analytical and experimental results is not as good for these tests as was found for the test with torsional restraint.

Figures C.7 to C.9 show the variation of brace force with applied load for two purlin line, three continuous 5 ft. span tests with torsional, third point and midspan restraint, respectively. For the torsional restraint case, Figures C.7(a), (c) and (d) show good correlation between the analytical and experimental total brace forces, external brace forces and internal brace forces, respectively. Although the correlation is not as good for the third point restraint test, Figures C.8(a), (c) and (d), or for the midspan restraint test, Figures C.9(a), (c) and (d), as it was for torsional restraint, it is still considered to be acceptable.

Model Test Results: A total of 28 quarter-scale tests were conducted by Seshappa [7] to study lateral restraint requirements for Z-purlin supported roof systems, these tests are grouped in a so called C test series. Four additional tests, designated the S test series, were conducted to examine the adequacy of the stiffness model when extreme values of purlin depth to span ratio are used. All three previously defined bracing configurations were considered in the C test series but only torsional restraint was used for the S test series. Purlin spacing was 1.25 ft. in all cases. The purlins used for the C test series were 2 in. deep with a 5 ft. span, these dimensions were varied for the S test series, see Table 3.1. Thirteen representative tests were selected for comparison with analytical predictions. Plots of analytical and experimental brace forces versus uniform applied load for these tests are found in Appendix C.

In Appendix C, Figure C.1 shows analytical and experimental variation of brace force with uniform load for a two purlin line, 5 ft. simple span test with torsional restraint braces. It is noted that the experimental brace force curve in Figure C.1 undergoes a considerable change in its slope near 7 plf of applied loading and then becomes nearly parallel to the analytical brace force curve as the load is increased until near failure. This is a characteristic of the experimental quarter-scale test curves and is due to the fact that the actual force in the brace cannot be determined until the pretensioning forces acting on that brace are totally overcome. Because of the small size of the brace members, it was reported by Seshappa [7] that it was very difficult to install the braces without initial slack or internal pretension. Being aware of this fact, it is concluded from Figure C.1 that

Figures B.1 and B.2 show the results of two 14 ft. single span tests. The first test was conducted with two purlin lines and the second using seven purlin lines. Agreement between analytical and experimental results is excellent for the two purlin test (Figure B.1). Agreement is very poor for the seven purlin test as the predicted percent brace force is more than twice as large as the experimental value. Of the nineteen sets of test results discussed herein, the results for this test were the only ones in which substantial disagreement existed between measured and predicted values. No reason was found for the discrepancy.

Shown in Figure B.3 are the results of a two purlin line, three continuous (20 ft.) spans test. Figure B.3(a) shows the relationship between applied load and the total brace force measured at the four brace locations. Figures B.3(c) and (d) show applied load versus brace force at the exterior and interior rafter locations, respectively. In all cases, agreement is excellent between analytical and experimental values.

Figure B.4 shows the results from a test of a two purlin line, 22 ft. single-span system with torsional restraint braces. The plot shown on Figure B.5 is for a six purlin line, 22 ft. single-span system with torsional restraints. Agreement between analytical and experimental results is excellent for both tests.

The last prototype test is a two purlin line, 20 ft. single span system with torsional restraint braces. Figure B.6 shows excellent agreement between analytical and experimental results for this test.

screws for prototype tests and machine screws for quarter scale tests. In most tests concrete blocks or clay brick units were placed on the panel to produce uniformly distributed loads on the purlins. For the remaining tests, suction was used to simulate uniform gravity loading. Calibrated dynamometers were used to measure brace forces as the load was incremented until failure of the system occurred. The reader is referred to References 5, 6 or 7 for more detailed information concerning testing procedures and the various test series.

A stiffness model was assembled for each full scale and quarter scale test and subsequently analyzed. The analytical results were available prior to testing for all quarter scale tests and were compared to experimental data obtained using a micro-computer based data acquisition system as the testing progressed. Of special interest was the measured restraint force and midspan vertical deflection.

Plots of load versus brace force for the six full scale tests are found in Appendix B and for the thirteen model tests in Appendix C. The ratio of total brace force to the total applied vertical load, expressed as a percent, was also examined. This ratio will be referred to as the "percent brace force" in the remainder of this thesis.

Prototype Results: Applied loading versus brace force from two purlin line, single span and multiple span, and six and seven purlin line, single span prototype tests are shown in Figures B.1 to B.6 in Appendix B. For all of these tests, only torsional braces were used and purlin spacing was 5 ft.

Table 3.1
Test Series and Configurations

Test Name	Test Type	Purlin depth (in)	Restraint configuration	Number of spans	Span (ft)	Number of purlin lines
a/2-3	Full Scale	8.0	Torsional	1	14.3	2
A/7-2	Full Scale	8.0	Torsional	1	14.0	7
3A/2-1	Full Scale	8.0	Torsional	3	20.0	2
B/2-1-A	Full Scale	8.0	Torsional	1	22.3	2
B/6-3	Full Scale	8.0	Torsional	1	22.0	6
III	Full Scale	8.0	Torsional	1	20.0	2
C/2-1	Quarter Scale	2.0	Torsional	1	5.0	2
C/6-1	Quarter Scale	2.0	Torsional	1	5.0	6
C/2-15	Quarter Scale	2.0	Third Point	1	5.0	2
C/2-16	Quarter Scale	2.0	Midspan	1	5.0	2
C/6-2	Quarter Scale	2.0	Third Point	1	5.0	6
C/6-3	Quarter Scale	2.0	Midspan	1	5.0	6
3C/2-1	Quarter Scale	2.0	Torsional	3	5.0	2
3C/2-4	Quarter Scale	2.0	Third Point	3	5.0	2
3C/2-3	Quarter Scale	2.0	Midspan	3	5.0	2
S1/2-15	Quarter Scale	1.5	Torsional	1	3.75	2
S1/2-25	Quarter Scale	1.5	Torsional	1	6.25	2
S4/2-15	Quarter Scale	3.0	Torsional	1	3.75	2
S4/2-25	Quarter Scale	3.0	Torsional	1	6.25	2

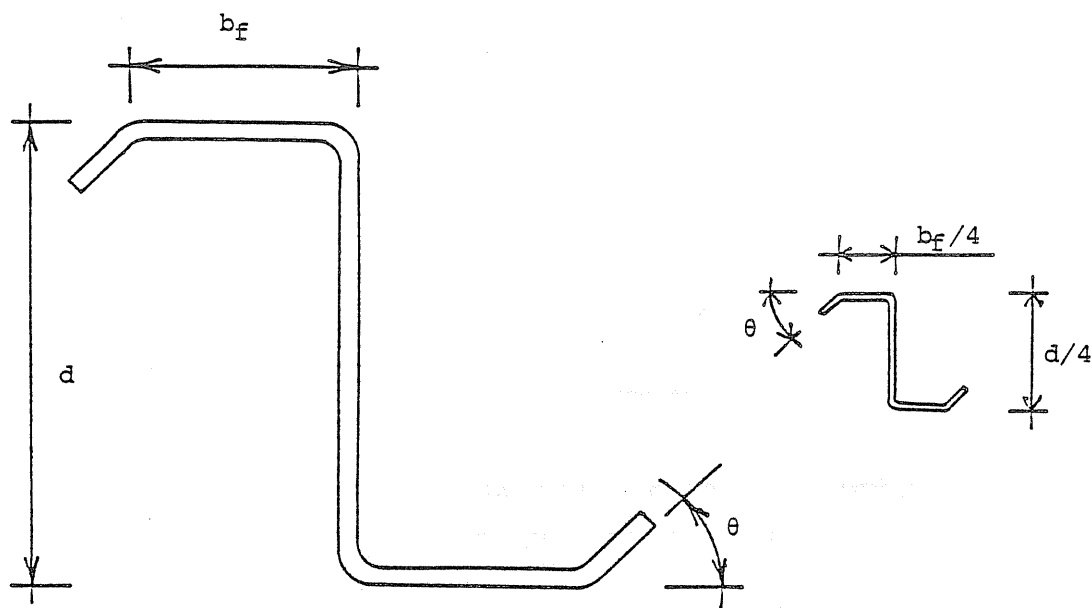


Figure 3.1 Typical Prototype and Model Cross Section

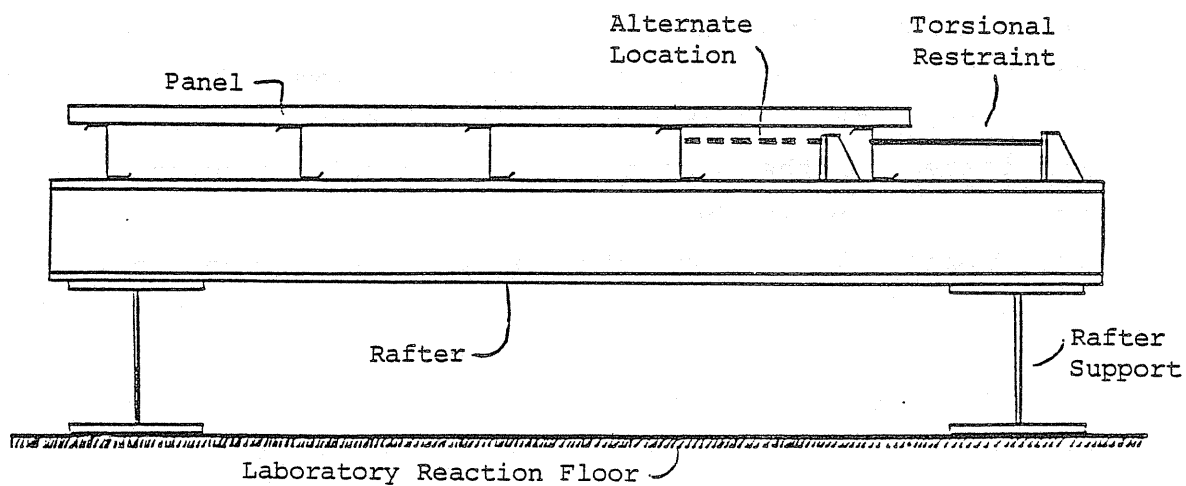


Figure 3.2 Typical Test Setup Cross Section

CHAPTER III

COMPARISON OF ANALYTICAL RESULTS WITH TEST RESULTS

3.1 Testing Configurations and Test Series

A number of full scale and quarter-scale tests were conducted in sister projects at the Fears Structural Engineering Laboratory, University of Oklahoma, to determine lateral restraint forces for Z-purlin supported roof systems [5,6,7]. The full-scale purlins used in the tests were industrial cold rolled Z-sections with 8 in. depth and material thickness varying between 0.075 in. and 0.09 in. The quarter-size press broken sections were fabricated at the Laboratory with depths between 1.5 in. and 3.0 in. using sheet material with a thickness of 0.025 in. Figure 3.1 shows the typical prototype and model cross-sections.

Results of six of the full scale and thirteen of the quarter scale tests were chosen for comparison purposes in this study. All of the tests were conducted to failure. Details of the test parameters are given in Table 3.1. Figure 3.2 shows an over all view of a typical test setup cross-section. The prototype purlins were bolted directly to pinned rafters; whereas, simple support conditions were provided for the quarter scale purlins. The corrugated steel panel was attached to the purlins using self drilling

TABLE 2.1

Comparison of Analytical Model Results
with Experimental Results

Test Type	Span ft.	<u>Lateral Restraint Forces</u> <u>Total Applied Vertical Load</u>		
		Stiffness Model	Ghazanfari [3]	Avg. Exp.
Full Scale	14.0	0.20	0.25	0.19
	20.0	0.22	0.26	0.22
Quarter Scale	5.0	0.21	0.30	0.24

by a triangle. The resultant load is then applied to the purlin at a distance $e = b_f/3$ from the plane of the web, Figure 2.8(b). The system is then analyzed for a uniformly distributed vertical load, w , and a uniformly distributed torque, (see Figure 2.8(c)), given by

$$M_x = w (b_f/3) \quad (2.2)$$

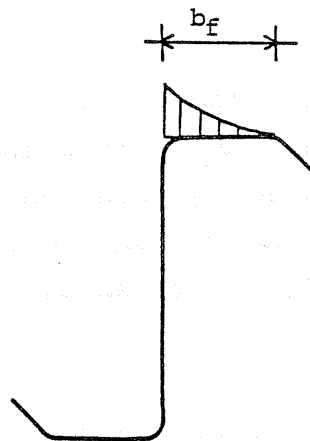
where b_f is the purlin flange width

2.3 Method of Solution

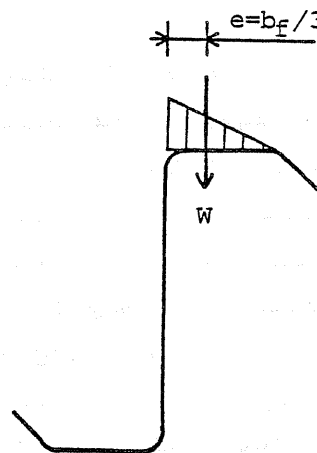
The computer software package called STRUDL (Structural Design Language), available on the IBM 3081 computer of the University of Oklahoma, was used to perform the analyses. A separate program to generate the data needed for the STRUDL package was written. Storage limitations of the available computer did not allow the analysis of more than twenty single-span purlin line systems or eight three-span purlin line systems. The CPU time varied from about four seconds for small systems to two minutes for the larger ones. Sample input data and results for a two purlin, single span Z-purlin system with torsional restraints at the rafters is given in Appendix A.

2.4 Comparison With Other Analytical Models

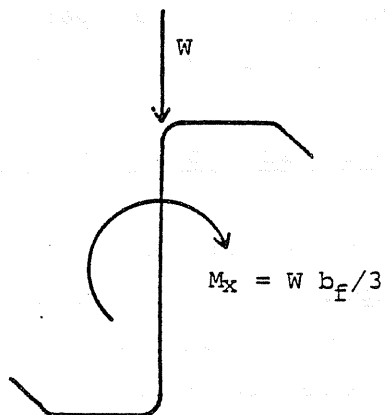
Lateral restraint forces obtained from the model were compared to those reported by Ghazanfari and Murray [3] and were found to be 10 to 20% smaller. However, when results from the two models were compared to experimental data, the results from the model proposed here were found to be in close agreement. Table 2.1 shows results from the analytical models and from laboratory tests. These results will be discussed in detail in Chapter III.



a) Probable Load Distribution

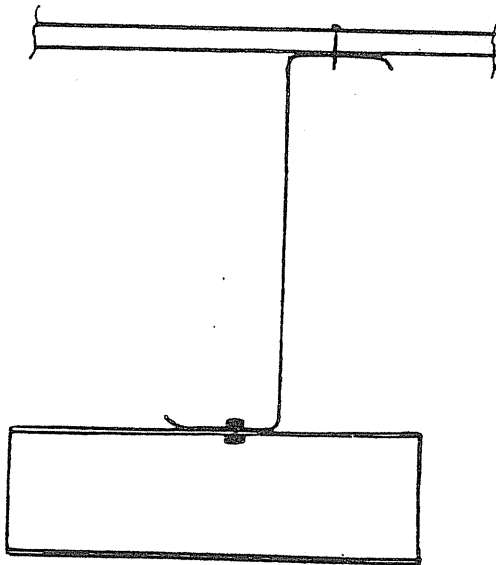
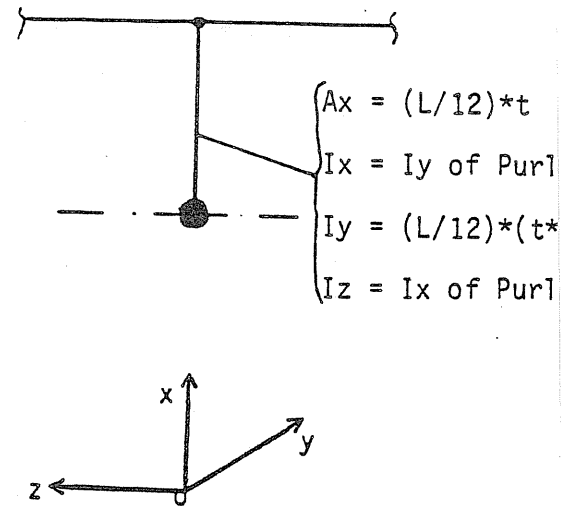
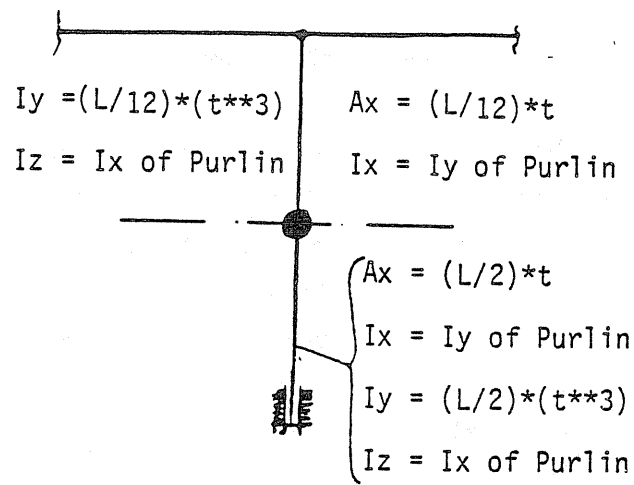


b) Linear approximation of Load Distribution

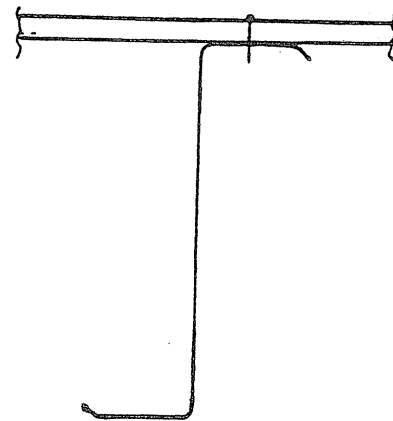


c) Analysis Load Configuration

Figure 2.8 Applied Purlin Load



At Rafter



At Mid-span

Figure 2.7 Purlin Cross-Section

2.2.4 Cross-Sectional Properties of the Purlin Members

As previously described, the purlin was modeled using two sets of space frame members as shown in Figure 2.5. The properties of these members were first determined based on the properties of the purlin itself and judgment. The so constructed model was then analyzed and results checked against experimental data from six full scale and five quarter scale tests that were available at the time. A few trials with various member properties were needed until good correlation between theoretical and experimental results was obtained. The final cross-sectional properties of the B-type members are given in Figure 2.7. They are specified according to the location of the member within the purlin, i.e., at rafter or at midspan.

The A-type members have the same properties as the purlin itself, except for the torsional constant I_x which is 10.0 in^4 for full scale systems and 0.625 in^4 for quarter scale systems. These relatively large values are needed since the B type members represent the entire torsional stiffness of the purlin and the panel-to-purlin connection.

2.2.5 Applied Load

Gravity loads are applied to the deck of the roof system which is attached to the purlins at their top flanges. These loads are then transmitted to the purlins eccentrically with respect to the shear center because of the nature of the load distribution on the flange which varies from zero at the lip location to a maximum at the web, see Figure 2.8(a). To simplify the problem, the distribution of the load across the flange is approximated

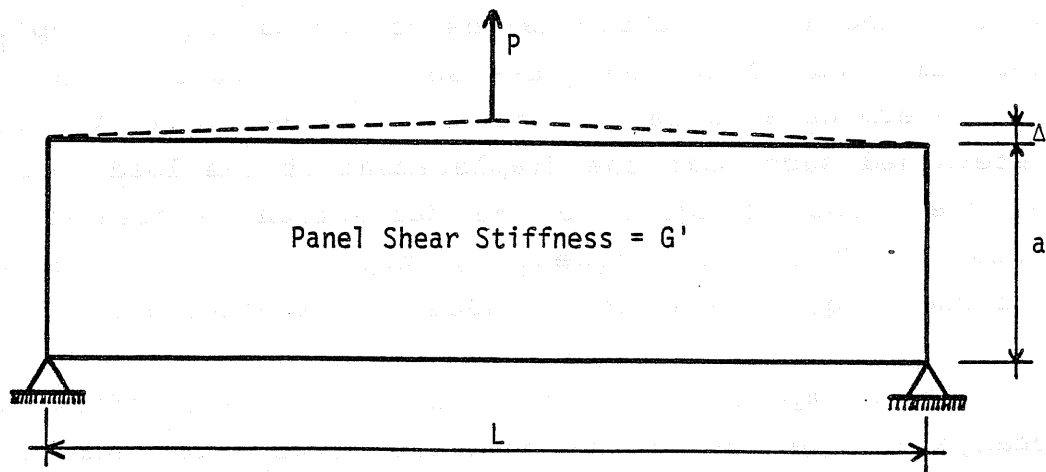
where L and a are the dimensions of the panel. By applying the same load P to the truss shown in Figure 2.6(b), one can determine a value for the truss member area, A , can be determined such that the displacement at the load location of the truss is equal to the deflection calculated from Equation 2.1. Consequently, the truss will have a stiffness equal to G' when loaded at its mid-span.

It is important to note, that the truss stiffness will change if the loading is changed. Ghazanfari and Murray [3] studied the variation of lateral forces with an increasing panel shear stiffness and found that the forces will increase from zero to a maximum as G' is increased from zero to approximately 1500 lbs/in and then remain nearly constant as G' is increased to infinity. Thus, it is assumed that the variation of truss stiffness can be disregarded if the actual panel shear stiffness is greater than 1500 lbs/in.

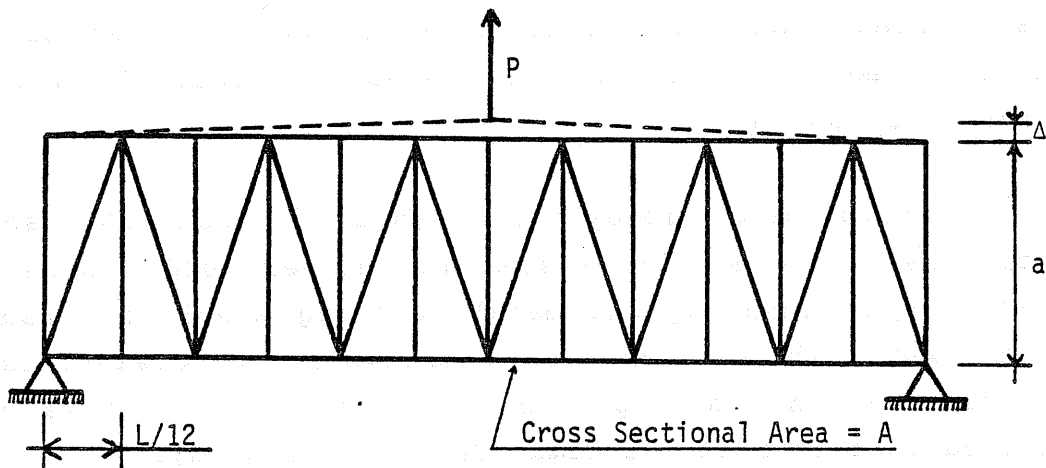
Curtis and Murray [6] reported that the shear stiffness of a decking system is between 1000 lbs/in and 3500 lbs/in when typical metal building steel roof panels are used with self-drilling fasteners as panel-to-panel connectors. An intermediate value of 2500 lbs/in is used for calculations in the remainder of this study.

2.2.3 Modeling of the Braces

Since brace members are only subjected to axial tensile force, they are represented by truss type line elements having the cross-sectional area of the brace itself.



a) Actual System



b) Stiffness Model

Figure 2.6 Panel Stiffness Model